(29) M. F. Farona, P. A. Lofgren, and P. S. Woon, *J. Chem. Soc., Chem. Commun.*, 246 (1974).
(30) M. A. Bennett, R. N. Johnson, G. B. Robertson, T. W. Turney, and P. O. Whimp, *Inorg. Chem.*, **15**, 97 (1976).
(31) (a) R. W. Kiser, M. A. Krassoi, and R. J. Clark, *J. Am. Chem. Soc.*, **89**, 3654 (1967); (b) R. E. Sullivan and R. W. Kiser, *Chem. Commun.*, 1425 (1968); (c) R. W. Kiser, M. A. Krassoi, and R. J. Clark, quoted by R. W. Kiser in "Characterization of Organometallic Compounds", M. Tsutsui, Ed., Interscience, New York, N.Y., 1969, Part 1, p 197.
(32) J. Lewis and B. F. G. Johnson, *Acc. Chem. Res.*, **1**, 245 (1968).
(33) R. K. Harris, *Can. J. Chem.*, **42**, 2275 (1964).
(34) G. Cetini, O. Gambino, P. L. Stanghellini, and G. A. Vaglio, *Inorg. Chem.*, **6**, 1225 (1967).
(35) F. A. Cotton, L. Kruczynski, B. L. Shapiro, and L. F. Johnson, *J. Am. Chem. Soc.*, **94**, 6191 (1972).
(36) J. G. Bullitt, F. A. Cotton, and T. J. Marks, *Inorg. Chem.*, **11**, 671 (1972); O. A. Gansow, A. R. Burke, and W. D. Vernon, *J. Am. Chem. Soc.*, **94**, 2550 (1972).
(37) R. D. Adams and F. A. Cotton, *J. Am. Chem. Soc.*, **94**, 6193 (1972); **95**, 6589 (1973); *Inorg. Chem.*, **13**, 249 (1974).
(38) Noise decoupling approximates a rate process: R. R. Ernst, *J. Chem. Phys.*, **45**, 3845 (1966). However it remains constant over the set of measurements, as is evident from the similar widths at half peak heights for the low- and high-temperature extremes, and it is nearly complete, as shown by the observed lorentzian line shapes. The broadness arising from incomplete decoupling can therefore be included in a constant T_2 which we use here to account for contributions to line width apart from the rate process under investigation.
(39) We discuss the barrier to exchange in terms of $\Delta G^‡$ rather than the enthalpy of activation, $\Delta H^‡$, or the activation energy, E_a, calculated from the Arrhenius equation. Although there is not a strict 1:1 correspondence, any errors should be common to all of the data and it is the *differences* which are significant.
(40) R. D. Adams and F. A. Cotton, *Inorg. Chim. Acta*, 7, 153 (1973); R. D. Adams, D. E. Collins, and F. A. Cotton, *J. Am. Chem. Soc.*, **96**, 749 (1974).
(41) J. P. Jesson and P. Meakin, *J. Am. Chem. Soc.*, **96**, 5760 (1974).
(42) R. S. Berry, *J. Chem. Phys.*, **32**, 933 (1960).
(43) I. Ugi, D. Marguarding, H. Klusacek, P. Gillespie, and F. Ramirez, *Acc. Chem. Res.*, **4**, 288 (1971).
(44) L. Kruczynski, L. K. K. Li Shing Man, and J. Takats, *J. Am. Chem. Soc.*, **96**, 4006 (1974); S. T. Wilson, N. J. Coville, J. R. Shapley, and J. A. Osborn, *ibid.*, **96**, 4038 (1974).
(45) L. Kruczynski and J. Takats, *J. Am. Chem. Soc.*, **96**, 932 (1974).
(46) C. G. Kreiter, S. Stüber, and L. Wackerle, *J. Organomet. Chem.*, **66**, C49 (1974).
(47) G. Rigatti, G. Boccalon, A. Ceccon, and G. Giacometti, *J. Chem. Soc. Chem. Commun.*, 1165 (1972).
(48) J. D. Warren and R. J. Clark, *Inorg. Chem.*, **9**, 373 (1970).
(49) J. D. Warren, M. A. Busch, and R. J. Clark, *Inorg. Chem.*, **11**, 452 (1972).
(50) M. A. Bennett, R. N. Johnson, and T. W. Turney, *Inorg. Chem.*, **15**, 111 (1976).

Contribution from the Research School of Chemistry,
The Australian National University, Canberra, A.C.T. 2600, Australia

Correlated Intermolecular and Intramolecular Ligand Exchange in μ-Acetylene-bis(ligand)tetrakis(trifluorophosphine)dirhodium Complexes and the Crystal and Molecular Structure of the Diphenylacetylene–Triphenylphosphine Derivative $Rh_2(PF_3)_4[P(C_6H_5)_3]_2(C_6H_5C_2C_6H_5)\cdot(C_2H_5)_2O$

M. A. BENNETT,* R. N. JOHNSON, G. B. ROBERTSON, T. W. TURNEY, and P. O. WHIMP

Received June 3, 1975 AIC50379S

The acetylene complexes $Rh_2(PF_3)_6(ac)$ (ac = $C_6H_5C_2C_6H_5$, $C_6H_5C_2CH_3$, or p-$NO_2C_6H_4C_2CO_2C_2H_5$) react with monodentate tertiary phosphines and arsines (L) to give disubstitution products $Rh_2(PF_3)_4L_2(ac)$ and with o-phenylenebis(dimethylarsine), o-$C_6H_4[As(CH_3)_2]_2$ (diars), to give $Rh_2(PF_3)_2(diars)_2(ac)$ (ac = $C_6H_5C_2C_6H_5$ or $C_6H_5C_2CH_3$). The reaction with monodentate ligands is reversed by the action of PF_3. The crystal and molecular structure of the diphenylacetylene–bis(triphenylphosphine) derivative [L = $P(C_6H_5)_3$; ac = $C_6H_5C_2C_6H_5$] has been determined by three-dimensional X-ray structural analysis using 6834 independent reflections, with $I/\sigma(I) \geq 3.0$, collected by counter methods. The complex crystallizes in the triclinic space group $P\bar{1}$ (C_i^1, No. 2) with a = 21.186 (9) Å, b = 12.994 (5) Å, c = 12.942 (5) Å, α = 114.10 (2)°, β = 64.36 (2)°, γ = 115.33 (2)°, and Z = 2. The structure was solved by conventional heavy-atom methods and was refined by block-diagonal least-squares methods to final weighted and unweighted R factors of 0.046 and 0.042, respectively. The molecule is structurally similar to cobalt–carbonyl–acetylene complexes such as $Co_2(CO)_6(\mu$-$C_6H_5C_2C_6H_5)$ and consists of two $[Rh(PF_3)_2[P(C_6H_5)_3]]$ moieties bridged by diphenylacetylene, the C≡C bond of which is above and approximately normal to the Rh–Rh axis. The triphenylphosphine groups are on the same side of the molecule as the bridging acetylene, and the Rh–Rh distance [2.740 (1) Å] is in the range expected for a rhodium–rhodium single bond. The ^{19}F NMR spectra of the disubstitution products containing unsymmetrical acetylenes, $Rh_2(PF_3)_4L_2(RC_2R')$, show signals due to PF_3 groups in two different environments at or just below room temperature, but on raising the temperature intramolecular PF_3 exchange takes place. This process appears to be initiated by dissociation of the tertiary phosphine or arsine (L). The free energies of activation, $\Delta G^‡$, for the intramolecular process have been estimated by approximate line shape analysis of the ^{19}F NMR spectra and are higher for the tertiary phosphine than for the tertiary arsine derivatives. In the one case studied, the electron-withdrawing acetylene ethyl p-nitrophenylpropiolate gives rise to a higher $\Delta G^‡$ than either diphenylacetylene or 1-phenylpropyne. Possible mechanisms involving the fluxional behavior of a coordinately unsaturated intermediate are discussed. A 1:1 mixture of $Rh_2(PF_3)_4[As(CH_3)(C_6H_5)_2]_2(C_6H_5C_2CH_3)$ and $Rh_2(PF_3)_6(C_6H_5C_2CH_3)$ undergoes intermolecular PF_3 exchange in the temperature range 50–82°, perhaps via a pentakis intermediate $Rh_2(PF_3)_5[As(CH_3)(C_6H_5)_2](C_6H_5C_2CH_3)$. The diars derivatives $Rh_2(PF_3)_2(diars)_2(ac)$ show temperature-independent ^1H and ^{19}F NMR spectra in the range −90° to room temperature, but their structure could not be determined unambiguously.

Introduction

In the previous paper,[1] we showed that octakis(trifluorophosphine)dirhodium, $Rh_2(PF_3)_8$, reacts with a variety of acetylenes (ac) to give bridging acetylene complexes $Rh_2(PF_3)_6(ac)$, the PF_3 groups of which undergo rapid intramolecular exchange at room temperature. The preparation of tertiary phosphine and arsine substitution products was undertaken in order to obtain crystalline derivatives suitable for X-ray structural analysis. It was also hoped that a study of their variable-temperature ^{19}F NMR spectra would assist in determining the mechanism of intramolecular exchange in the parent compounds. This paper reports the preparation and ligand-exchange behavior of the substitution products, together with a single-crystal X-ray analysis of the diphenylacetyl-

Table I. Elemental Analyses and Melting Points

		% calcd				% found			
Compd[a]	Mp, °C	C	H	P	Other	C	H	P	Other
$Rh_2(PF_3)_4[P(C_6H_5)_3]_2(C_6H_5C_2C_6H_5)$	110–113[b]	47.6	3.7	14.7		47.1	3.6	14.1	
$Rh_2(PF_3)_4[P(C_6H_5)_3]_2(C_6H_5C_2C_6H_5)\cdot(C_2H_5)_2O$	164–165[b]	48.6	3.8	13.9		48.8	3.9	13.3	
$Rh_2(PF_3)_4[As(C_6H_5)_3]_2(C_6H_5C_2C_6H_5)$	189[b]	44.5	3.0	9.2	11.1 (As)	44.1	3.2	8.7	10.8 (As)
$Rh_2(PF_3)_4[P(CH_3)(C_6H_5)_2]_2(C_6H_5C_2C_6H_5)$	146–148	42.3	3.2	16.3		42.8	3.5	16.1	
$Rh_2(PF_3)_4[P(C_6H_5)_3]_2(C_6H_5C_2CH_3)$	147–151[b]	45.1	3.2	15.5		44.5	3.3	15.3	
$Rh_2(PF_3)_4[As(C_6H_5)_3]_2(C_6H_5C_2CH_3)$	176–180	42.6	3.0			42.9	3.2		
$Rh_2(PF_3)_4[P(CH_3)(C_6H_5)_2]_2(C_6H_5C_2CH_3)$	105	39.1	3.2	17.3		39.4	3.5	17.0	
$Rh_2(PF_3)_4[As(CH_3)(C_6H_5)_2]_2(C_6H_5C_2CH_3)$	136–138	36.2	3.0		12.9 (As)	36.8	3.4		12.9 (As)
$Rh_2(PF_3)_4[As(C_6H_5)_3]_2(p\text{-}O_2NC_6H_4C_2CO_2C_2H_5)$	174[b]	40.6	2.8		10.8 (As), 1.0 (N)	40.6	3.1		10.8 (As), 1.0 (N)
$Rh_2(PF_3)_2(diars)_2(C_6H_5C_2C_6H_5)$[c]	196[b]	36.1	3.7		26.5 (As)	35.6	3.9		26.1 (As)
$Rh_2(PF_3)_2(diars)_2(C_6H_5C_2CH_3)$[c]	180–183[b]	32.6	3.8			32.7	3.9		

[a] Each compound was dark red to burgundy in color. [b] Melted with decomposition. [c] diars = $o\text{-}C_6H_4[As(CH_3)_2]_2$.

ene–bis(triphenylphosphine) derivative, $Rh_2(PF_3)_4[P(C_6H_5)_3]_2(C_6H_5C_2C_6H_5)\cdot(C_2H_5)_2O$. A preliminary account of the structure analysis has appeared elsewhere.[2]

Experimental Section

Experimental, spectroscopic, and line-shape fitting procedures are as previously described.[1] Analytical data and melting points are in Table I. The following preparations are representative of the procedures used.

μ-Diphenylacetylene-bis(triphenylphosphine)tetrakis(trifluorophosphine)dirhodium(0)(*Rh–Rh*) Monoetherate, $Rh_2(PF_3)_4[P(C_6H_5)_3]_2(C_6H_5C_2C_6H_5)\cdot(C_2H_5)_2O$. A solution of $Rh_2(PF_3)_6(C_6H_5C_2C_6H_5)$ (0.09 g)[1] in diethyl ether (5 ml) was treated with triphenylphosphine (0.20 g, excess). After 1–2 min the solution was filtered to remove undissolved ligand. After 30 min the filtrate had turned dark red and, on keeping at −5°, slowly deposited burgundy-colored crystals. These were collected and dried in vacuo to give 0.06 g (46%) of the required product.

The unsolvated complex was obtained by carrying out the reaction in *n*-pentane.

μ-1-Phenylpropyne-bis(diphenylmethylarsine)tetrakis(trifluorophosphine)dirhodium(0)(*Rh–Rh*), $Rh_2(PF_3)_4[As(CH_3)(C_6H_5)_2]_2(CH_3C_2C_6H_5)$. Diphenylmethylarsine (0.30 g, excess) in *n*-pentane (10 ml) was added to a solution of $Rh_2(PF_3)_6(CH_3C_2C_6H_5)$ (0.21 g) in *n*-pentane (15 ml) under nitrogen. The solution rapidly turned dark red and, after a small amount of flocculent buff precipitate had been filtered off, was kept at −10° for 2 days. The burgundy-colored crystals were washed with three 10-ml portions of *n*-pentane and dried in vacuo to give 0.18 g (63%) of the required product.

Collection and Reduction of X-Ray Intensity Data. Approximate unit cell dimensions for crystals of $Rh_2(PF_3)_4[P(C_6H_5)_3]_2(C_6H_5C_2C_6H_5)\cdot(C_2H_5)_2O$ were obtained from preliminary Weissenberg (0*kl*, 1*kl* data) and precession (*h*0*l*, *h*1*l*, *hk*0, *hk*1 data) photographs which showed no evidence of diffraction symmetry higher than C_i ($\bar{1}$). The choice of the centrosymmetric triclinic space group $P\bar{1}$ (C_i^1, No. 2) has been confirmed by the successful solution and refinement of the structure.

The crystal chosen for data collection was transferred to a Picker FACS-I fully automatic four-circle diffractometer, and was aligned with the crystal *a* axis and the instrumental Φ axis approximately coincidental. Accurate cell dimensions and crystal orientation matrix, together with their estimated standard errors, were obtained from the least-squares refinement[3] of the 2θ, ω, χ, and Φ values obtained for 12 carefully centered high-angle reflections (2θ > 83°). Full details of the crystal data are listed in Table II.

Details of the experimental conditions and data collection methods used are outlined in Table III. During data collection, the intensities of the three "standard" reflections showed a regular, time-dependent decrease of 7%. Crystal decomposition was assumed to be isotropic and independent of 2θ; before further calculation the intensity data were corrected accordingly.

Reflection intensities were reduced to values of $|F_o|$,[4] and each reflection was assigned an individual estimated standard deviation $[\sigma(F_o)]$.[4] For this data set, the instrumental "uncertainty" factor (ρ)[5] was assigned a value of $0.001^{1/2}$. Reflection data were sorted, equivalent reflections were averaged, reflections with $I/\sigma(I) < 3.0$ were discarded as being unobserved,[4] and those reflections for which the individual background measurements differed significantly (i.e., $\geq 4.0\sigma$)[4] were also discarded. The statistical *R* factor (R_s)[4] for the

Table II. Crystal Data for $Rh_2(PF_3)_4[P(C_6H_5)_3]_2(C_6H_5C_2C_6H_5)\cdot(C_2H_5)_2O$[a]

a = 21.186 (9) Å[b,c]	α = 114.10 (2)°
b = 12.994 (5) Å	β = 64.36 (2)°
c = 12.942 (5) Å	γ = 115.33 (2)°
Crystal color deep red	Formula $C_{50}H_{40}F_{12}P_6Rh_2\cdot(C_2H_5)_2O$
Mol wt 1334.6	Cell vol 2792.2 Å^3
ρ_{obsd} = 1.57 (1) g cm^{-3}	ρ_{calcd} = 1.59 g cm^{-3}
Space group $P\bar{1}$ (C_i^1, No. 2)	Z = 2
Crystal dimensions 0.030 × 0.007 × 0.010 cm[d]	μ(Cu Kα) = 71.45 cm^{-1}

[a] Cell dimensions were measured at 20 ± 1°C. [b] Estimated standard deviations (in parentheses) in this and the following tables, and also in the text, refer to the least significant digit(s) in each case. [c] The "reduced" cell, obtained from a Delaunay reduction [B. Delaunay, *Z. Kristallogr., Kristallgeom., Kristallphys., Kristallchem.*, 84, 109 (1933)] is a' = 12.994 Å, b' = 19.470 Å, c' = 12.942 Å, α' = 101.18°, β' = 114.10°, γ' = 101.19°, cell volume 2792.2 Å^3. [d] Crystal dimensions are parallel to a^*, b^*, and c^*, respectively.

Table III. Details of X-Ray Data Collection

Radiation	Cu Kα
Wavelength	1.5418 Å
Monochromator	Graphite crystal
Tube takeoff angle	3.0°
Crystal to counter distance	28.5 cm
Scan technique	θ–2θ scans
Scan speed	2°/min
Scan width	From 0.95° below the Cu Kα_1 maximum to 0.95° above the Cu Kα_2 maximum of each peak
Scan range limits	3° ≤ 2θ ≤ 125°
Total background counting time[a]	20 sec
"Standard" reflection indices[b]	(054), (803), (06$\bar{5}$)
Crystal stability	7% isotropic decay
Form of data collected	*hkl*, *hk*$\bar{l}$, *h*$\bar{k}$*l*, *h*$\bar{k}\bar{l}$
Total data collected	9929
No. with $I/\sigma(I) \geq 3.0$	6834
No. with $I/\sigma(I) \geq 6.0$	5765

[a] Backgrounds were counted on either "side" of each reflection (10 sec each side) at the scan width limits and were assumed to be linear between these two points. [b] The three "standard" reflections were monitored after each 40 measurements throughout data collection.

6834 reflections of the terminal data set was 0.026.

To conserve computing time, the structure was initially solved and refined using data for which $I/\sigma(I) \geq 6.0$ (5765 reflections).

Solution and Refinement of the Structure. A three-dimensional Patterson map showed the positions of the two rhodium atoms and the six phosphorus atoms. The remaining atoms of the molecule were located from successive difference Fourier syntheses. The structure was refined by block-diagonal least-squares methods to final unweighted and weighted *R* factors of 0.042 (*R*) and 0.046 (R_w), respectively. Atomic scattering factors for the nonhydrogen atoms were taken from ref 6; those for Rh, P, and F were corrected for the real and imaginary parts of anomalous scattering.[7,8]

Table IV. Details of Least-Squares Refinement

Set no.	Conditions	No. of reflections	$I/\sigma(I)$	No. of cycles	R^a	R_w
1	All atoms isotropic; hydrogen atoms not included; equal (unit) weights	5765	6.0	3	0.091	0.099
2	At this stage, reflection data were corrected for absorption effects[b] All atoms isotropic; hydrogen atoms not included; individual weights[c] were used in these and all subsequent cycles	6834	3.0	6	0.091	0.112
3	All atoms anisotropic;[d] hydrogen atoms not included	6834	3.0	6	0.051	0.060
4	All nonhydrogen atoms anisotropic; fixed isotropic hydrogen atom contributions included	6834	3.0	6	0.042	0.046

[a] $R = \Sigma||F_o| - |F_c||/\Sigma|F_o|$ and $R_w = \{\Sigma w[|F_o| - |F_c|]^2/\Sigma w/F_o|^2\}^{1/2}$, where $|F_o|$ is the observed and $|F_c|$ is the calculated structure factor and w is the weight. The function minimized throughout the least-squares process was $\Sigma w(|F_o| - |F_c|)^2$. [b] A grid of 20 × 6 × 8 points (parallel to a^*, b^*, and c^*, respectively) was used. The transmission factor (applied to $|F_o|^2$) ranged from 0.406 to 0.723. [c] Individual weights were of the form $[\sigma(F_o)]^{-2}$. [d] The anisotropic temperature factor takes the form $\exp[-(\beta_{11}h^2 + \beta_{22}k^2 + \beta_{33}l^2 + 2\beta_{12}hk + 2\beta_{13}hl + 2\beta_{23}kl)]$.

When fixed phenyl hydrogen atom contributions were included in the scattering model, it was assumed that the C–H distances were 1.087 Å. The phenyl hydrogen atoms were assigned fixed isotropic temperature factors 10% greater than the equivalent isotropic temperature factor of the carbon atoms to which they were bonded (i.e., $B_H = 1.1B_C$ Å^2). The hydrogen atom coordinates and temperature factors were recalculated prior to each refinement cycle. Scattering factors for hydrogen atoms were taken from the tabulation of Stewart et al.[9] No attempt was made to include the hydrogen atoms of the solvent ether molecule in the scattering model. A full account of the course of refinement is given in Table IV.

On the final refinement cycle, no individual parameter shift was greater than 0.1 of the corresponding parameter esd (estimated standard deviations derive from inversion of the block-diagonal matrices). A final electron density difference map showed no unusual features, and there were no positive maxima greater than 0.4 e/Å^3. The standard deviation of an observation of unit weight, defined as $[\sum w(|F_o| - |F_c|)^2/(m - n)]^{1/2}$ [where m is the number of observations and n (=676) is the number of parameters varied], is 1.72; cf. a value of 1.0 expected for ideal weighting. An examination of F_o and F_c shows no evidence of serious extinction effects, and there is no serious dependence of the minimized function on either $|F_o|$ or $\lambda^{-1} \sin\theta$.

Final atomic positional and thermal parameters, together with their estimated standard deviations (where appropriate), are listed in Tables Va and Vb. A listing of observed and calculated structure factor amplitudes [×10 (electrons)] is available (see the paragraph at the end of paper regarding supplementary material).

Computer Programs. The data reduction (SETUP), sorting (SORTIE), Fourier (ANUFOR), block-diagonal least-squares (BLKLSO), and absorption correction (ACACA) programs have been described elsewhere.[10] The figures were produced using ORTEP.[11] All calculations were carried out on the CDC3600 computer of the CSIRO Division of Computing Research, Canberra, and the Univac-1108 computer of The Australian National University Computer Centre.

Results and Discussion

Chemistry. The acetylene complexes $Rh_2(PF_3)_6(ac)$ (ac = $C_6H_5C_2C_6H_5$, $C_6H_5C_2CH_3$, or p-$NO_2C_6H_4C_2CO_2C_2H_5$) react with tertiary phosphines or arsines (L) at room temperature to give red, crystalline disubstitution products $Rh_2(PF_3)_4L_2(ac)$, while with the bidentate ligand o-phenylenebis(dimethylarsine), o-$C_6H_4[As(CH_3)_2]_2$ (diars), red disubstitution products $Rh_2(PF_3)_2(diars)_2(ac)$ (ac = $C_6H_5C_2C_6H_5$ or $C_6H_5C_2CH_3$) are obtained. The reaction seems to be general, but only those complexes containing arylacetylenes and diaryl-substituted ligands could be isolated. Although the complex with ac = $CH_3C_2CH_3$ and L = $P(C_6H_5)_3$ was identified by NMR spectroscopy, derivatives containing dialkylacetylenes or dimethylphenylphosphine were not obtained in a pure state and have not been studied further. The substitution reactions are similar to those of the analogous $Co_2(CO)_6(ac)$ complexes but occur even more readily; e.g., the formation of mono- and bis(triphenylphosphine) derivatives from $Co_2(CO)_6(C_6H_5C_2C_6H_5)$ is reported to require heating to 70°.[12] We have been unable to isolate monosubstitution products such as $Rh_2(PF_3)_5[P(C_6H_5)_3](C_6H_5C_2C_6H_5)$, although analogous $Co_2(CO)_5$ complexes are known.[12,13]

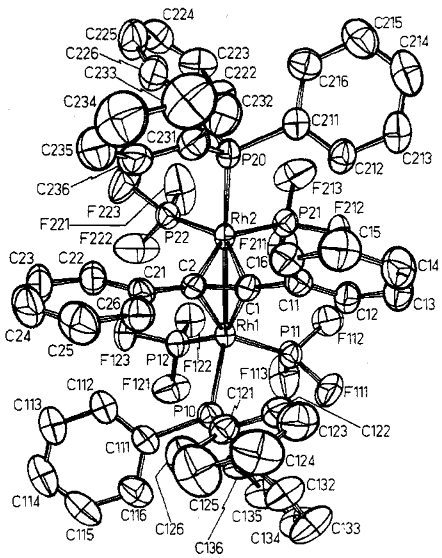

Figure 1. Overall stereochemistry of one molecule of $Rh_2(PF_3)_4[P(C_6H_5)_3]_2(C_6H_5C_2C_6H_5)$, together with the atom-numbering scheme.

Reaction of $Rh_2(PF_3)_6(C_6H_5C_2C_6H_5)$ with 1 equiv of triphenylphosphine gives the bis(ligand) derivative as the only isolable product, and there is no evidence for the presence of the monosubstitution product in a 1:1 mixture of $Rh_2(PF_3)_6(C_6H_5C_2C_6H_5)$ and $Rh_2(PF_3)_4[P(C_6H_5)_3]_2(C_6H_5C_2C_6H_5)$. However, the derivative $Rh_2(PF_3)_5[As(CH_3)(C_6H_5)_2](C_6H_5C_2CH_3)$ may be present in a 1:1 mixture of $Rh_2(PF_3)_4[As(CH_3)(C_6H_5)_2]_2(C_6H_5C_2CH_3)$ and $Rh_2(PF_3)_6(C_6H_5C_2CH_3)$ above 50° (see below).

Description of the Structure of $Rh_2(PF_3)_4[P(C_6H_5)_3]_2(C_6H_5C_2C_6H_5)\cdot(C_2H_5)_2O$. The crystal structure, as defined by the unit cell dimensions, symmetry operations, and atom coordinates of Tables Va and Vb, consists of discrete monomeric molecular units which have approximate C_2 symmetry about an axis through the midpoints of both the acetylene and rhodium–rhodium bonds.

The molecule consists of two $Rh(PF_3)_2[P(C_6H_5)_3]$ moieties bridged by a diphenylacetylene molecule, the C≡C bond of which is above and approximately normal to the Rh–Rh axis. The atom numbering scheme is shown in Figure 1, and a perspective view of the molecule is shown by the stereopairs of Figure 2. The contents of one unit cell are shown by the stereopairs of Figure 3. In each of these figures, the thermal ellipsoids (where shown) have been drawn to include 50% of the probability distribution, and, for clarity, the hydrogen atoms have been omitted.

Principal bond distances and interbond angles, together with their estimated standard deviations, are listed in Table VI, while bond distances and angles within the six triphenyl-

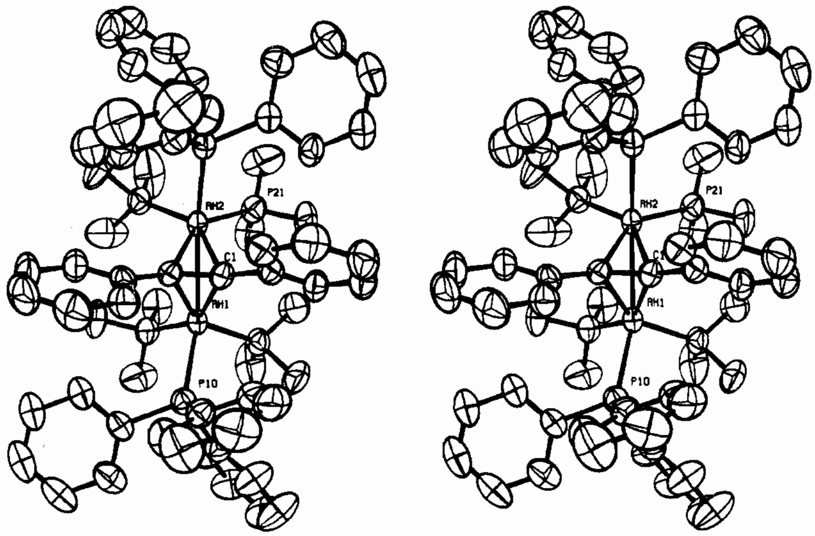

Figure 2. Stereoscopic view of the molecule.

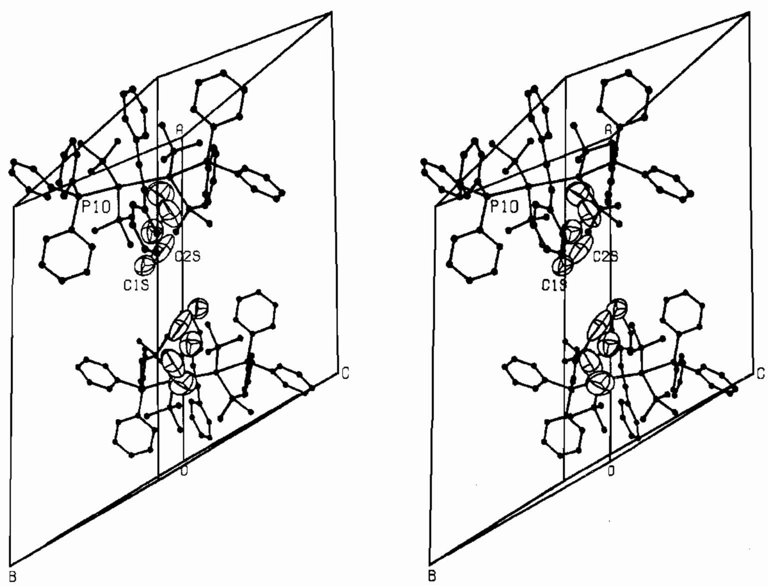

Figure 3. Stereoscopic view of the contents of one unit cell. Only the thermal ellipsoids for the solvent molecule have been drawn to include 50% of the probability distribution. The sequence of atoms in the solvent molecule is C(1S)–C(2S)–O(1S)–C(3S)–C(4S).

phosphine phenyl rings are listed in Table VII. The results of weighted least-squares planes calculations[14] are collected in Table VIII, and some important torsion angles are listed in Table IX.

Many features of the geometry of the $Rh_2(PF_3)_4[P(C_6H_5)_3]_2(C_6H_5C_2C_6H_5)$ molecule are similar to those observed for the cobalt carbonyl derivatives $Co_2(CO)_6(C_6H_5C_2C_6H_5)$,[15] $Co_2(CO)_6(C_6F_6)$[16] (C_6F_6 = hexafluoro-1-en-3-yne), and related molecules.[17–20] Thus, the angles Rh–Rh–P(triphenylphosphine) average 148.7°, compared with an average value of 148.1° found for the two corresponding Co–Co–C angles in $Co_2(CO)_6(C_6F_6)$[16] (i.e., the Co–Co–C angles on the same "side" of the molecule as the bridging diphenylacetylene group). In contrast, the Rh–Rh–P(PF_3) angles average 104.5°; cf. 100.3° (average) for the corresponding Co–Co–C angles in $Co_2(CO)_6(C_6F_6)$[16] and an average value of 101° for those of $Co_2(CO)_6(C_6H_5C_2C_6H_5)$.[15]

The acetylenic carbon–carbon distance in the bridging diphenylacetylene group [C(1)–C(2) = 1.369 (7) Å] is significantly longer than that expected for free acetylenes [1.206 (5) Å],[21] and it is also longer than the distance found for acetylenes which are coordinated to only one metal atom (ca. 1.29 Å).[22] The present distance is, however, in excellent agreement with that observed for $Co_2(CO)_6(C_6H_5C_2C_6H_5)$, which was originally reported as 1.46 Å[15] but was subsequently refined to 1.369 Å.[23] A similar distance [1.36 (3) Å] has also been found for the bridging carbon–carbon bond length in $Co_2(CO)_6(C_6F_6)$.[16]

The angles C(2)–C(1)–C(11) and C(1)–C(2)–C(21) [141.1 (5) and 141.5 (5)°, respectively] are equal within experimental error (3.0σ) but are significantly different from the value of 180° normally expected for the C≡C—C angle in "free" acetylenes. Surprisingly the present bond angles do not differ appreciably from those in $Pt[P(C_6H_5)_3]_2(C_6H_5C_2C_6H_5)$ [average 141°][24] despite the fact that the C≡C distance in the present complex is ca. 0.05 Å greater than that in the Pt(0) derivative [1.32 (9) Å].[24]

The distances C(1)–C(11) and C(2)–C(21) [1.459 (7) and 1.460 (7) Å, respectively] are equal within experimental error and are similar to the value of 1.46 Å expected for carbon–carbon single bonds between sp^2 and sp (approaching sp^2) hybridized atoms.[25] Within the two phenyl rings of the diphenylacetylene moiety, the bond lengths and bond angles appear normal and average 1.388 Å and 120.0°, respectively. The dihedral angle between these two phenyl rings is 42.1°.

The distances Rh(1)–C(1) and Rh(2)–C(2) [2.097 (5) and

Table Va. Refined Atomic Positional and Thermal Parameters for $Rh_2(PF_3)_4[P(C_6H_5)_3]_2(C_6H_5C_2C_6H_5)\cdot(C_2H_5)_2O$

ATOM	X	Y	Z	BETA11	BETA22	BETA33	BETA12	BETA13	BETA23
RH(1)	0.20705(2)	-0.05578(3)	0.17477(3)	0.00199(1)	0.00612(3)	0.00608(3)	0.00140(2)	-0.00124(2)	0.00085(3)
RH(2)	0.26029(2)	0.09562(3)	0.03778(3)	0.00188(1)	0.00522(3)	0.00690(3)	0.00109(1)	-0.00141(2)	0.00078(3)
P(10)	0.18664(8)	-0.24633(12)	0.18759(12)	0.00266(5)	0.00664(11)	0.00749(12)	0.00146(6)	-0.00154(6)	0.00158(9)
P(11)	0.10022(8)	-0.03385(14)	0.30856(14)	0.00265(5)	0.01094(15)	0.00840(13)	0.00273(7)	-0.00050(7)	0.00281(12)
P(12)	0.27408(8)	0.04377(13)	0.29693(13)	0.00306(5)	0.00855(13)	0.00790(13)	0.00143(7)	-0.00234(7)	0.00102(11)
P(20)	0.29265(7)	0.12176(11)	-0.15308(12)	0.00212(4)	0.00594(11)	0.00757(12)	0.00122(5)	-0.00133(6)	0.00135(9)
P(21)	0.18234(8)	0.20100(13)	0.13524(14)	0.00298(5)	0.00766(13)	0.00970(14)	0.00249(7)	-0.00069(7)	0.00160(11)
P(22)	0.35892(8)	0.23646(13)	0.08138(14)	0.00274(5)	0.00730(13)	0.01051(15)	0.00040(6)	-0.00280(7)	0.00217(11)
F(111)	0.0294(2)	-0.1418(4)	0.3166(4)	0.0024(1)	0.0157(5)	0.0218(6)	0.0014(2)	-0.0002(2)	0.0094(4)
F(112)	0.0628(2)	0.0440(4)	0.3080(4)	0.0042(2)	0.0184(5)	0.0222(6)	0.0060(2)	0.0016(3)	0.0107(5)
F(113)	0.0905(2)	0.0087(5)	0.4418(3)	0.0057(2)	0.0345(8)	0.0073(3)	0.0086(4)	-0.0001(2)	0.0011(4)
F(121)	0.2592(2)	0.0018(4)	0.4043(3)	0.0073(2)	0.0171(5)	0.0131(4)	-0.0006(3)	-0.0066(3)	0.0065(4)
F(122)	0.2723(2)	0.1714(3)	0.3701(3)	0.0056(2)	0.0089(3)	0.0135(4)	0.0025(2)	-0.0046(2)	-0.0036(3)
F(123)	0.3586(2)	0.0696(3)	0.2552(3)	0.0028(1)	0.0151(4)	0.0155(5)	0.0016(2)	-0.0036(2)	0.0013(4)
F(211)	0.1705(2)	0.2619(3)	0.2693(3)	0.0050(2)	0.0150(5)	0.0107(4)	0.0047(2)	-0.0019(2)	-0.0039(3)
F(212)	0.0999(2)	0.1483(3)	0.1445(3)	0.0028(1)	0.0174(5)	0.0151(4)	0.0041(2)	-0.0013(2)	0.0035(4)
F(213)	0.1949(3)	0.3121(4)	0.1026(4)	0.0074(2)	0.0155(5)	0.0259(7)	0.0080(3)	0.0041(3)	0.0119(5)
F(221)	0.3628(3)	0.3650(3)	0.1287(6)	0.0066(2)	0.0062(3)	0.0412(10)	0.0012(2)	-0.0110(4)	-0.0029(5)
F(222)	0.3921(3)	0.2380(4)	0.1653(5)	0.0082(3)	0.0228(7)	0.0312(8)	-0.0069(3)	-0.0134(4)	0.0173(6)
F(223)	0.4341(2)	0.2580(4)	-0.0164(4)	0.0026(1)	0.0211(6)	0.0185(6)	-0.0012(2)	-0.0021(2)	0.0059(5)
C(1)	0.2017(3)	-0.0884(4)	0.0057(4)	0.0021(2)	0.0056(4)	0.0062(4)	0.0009(2)	-0.0013(2)	0.0008(3)
C(2)	0.2729(3)	-0.0694(4)	-0.0060(4)	0.0022(2)	0.0058(4)	0.0063(4)	0.0009(2)	-0.0012(2)	0.0016(3)
C(11)	0.1482(3)	-0.1563(4)	-0.0591(4)	0.0026(2)	0.0055(4)	0.0079(5)	0.0006(2)	-0.0023(2)	0.0016(4)
C(12)	0.0740(3)	-0.1650(5)	-0.0019(5)	0.0023(2)	0.0077(5)	0.0094(5)	0.0010(2)	-0.0020(3)	0.0019(4)
C(13)	0.0236(3)	-0.2267(5)	-0.0650(6)	0.0029(2)	0.0102(6)	0.0133(7)	0.0008(3)	-0.0032(3)	0.0033(5)
C(14)	0.0469(4)	-0.2787(5)	-0.1851(6)	0.0039(3)	0.0105(6)	0.0141(8)	0.0002(3)	-0.0051(4)	0.0029(6)
C(15)	0.1206(4)	-0.2700(5)	-0.2445(5)	0.0046(3)	0.0083(6)	0.0093(6)	0.0010(3)	-0.0038(3)	0.0002(5)
C(16)	0.1709(3)	-0.2098(4)	-0.1812(5)	0.0032(2)	0.0070(5)	0.0073(5)	0.0013(3)	-0.0020(3)	0.0010(4)
C(21)	0.3322(3)	-0.1232(4)	-0.0735(4)	0.0028(2)	0.0067(4)	0.0068(4)	0.0025(2)	-0.0006(2)	0.0018(4)
C(22)	0.4041(3)	-0.0598(5)	-0.0676(5)	0.0025(2)	0.0101(6)	0.0107(6)	0.0020(3)	-0.0014(3)	0.0029(5)
C(23)	0.4594(3)	-0.1111(6)	-0.1292(6)	0.0027(2)	0.0144(8)	0.0117(7)	0.0037(3)	-0.0007(3)	0.0033(6)
C(24)	0.4448(4)	-0.2276(6)	-0.1987(6)	0.0045(3)	0.0160(8)	0.0129(8)	0.0061(4)	0.0000(4)	0.0041(7)
C(25)	0.3747(4)	-0.2922(5)	-0.2050(6)	0.0053(3)	0.0095(6)	0.0109(7)	0.0046(4)	-0.0015(4)	0.0000(5)
C(26)	0.3185(3)	-0.2401(5)	-0.1433(5)	0.0034(2)	0.0080(5)	0.0077(5)	0.0027(3)	-0.0009(3)	0.0010(4)
C(111)	0.2616(3)	-0.2703(5)	0.2005(5)	0.0034(2)	0.0078(5)	0.0082(5)	0.0025(3)	-0.0020(3)	0.0012(4)
C(112)	0.3337(3)	-0.2108(5)	0.1467(5)	0.0035(2)	0.0107(6)	0.0108(6)	0.0031(3)	-0.0021(3)	0.0021(5)
C(113)	0.3914(4)	-0.2359(6)	0.1459(6)	0.0037(3)	0.0144(8)	0.0140(8)	0.0040(4)	-0.0023(4)	0.0029(6)
C(114)	0.3785(4)	-0.3201(6)	0.1944(6)	0.0052(3)	0.0161(9)	0.0131(8)	0.0059(4)	-0.0036(4)	0.0008(6)
C(115)	0.3091(4)	-0.3809(6)	0.2457(6)	0.0067(4)	0.0124(7)	0.0136(8)	0.0053(4)	-0.0043(4)	0.0023(6)
C(116)	0.2484(4)	-0.3576(6)	0.2507(6)	0.0052(3)	0.0107(6)	0.0124(7)	0.0028(4)	-0.0037(4)	0.0031(5)
C(121)	0.1657(3)	-0.3712(4)	0.0611(4)	0.0027(2)	0.0066(4)	0.0073(5)	0.0011(2)	-0.0013(3)	0.0017(4)
C(122)	0.1102(3)	-0.3807(5)	0.0230(5)	0.0032(2)	0.0069(5)	0.0097(6)	0.0006(3)	-0.0022(3)	0.0028(4)
C(123)	0.0934(4)	-0.4724(5)	-0.0745(6)	0.0044(3)	0.0094(6)	0.0117(7)	0.0000(3)	-0.0042(4)	0.0031(5)
C(124)	0.1296(4)	-0.5557(6)	-0.1309(6)	0.0066(4)	0.0091(6)	0.0109(7)	0.0024(4)	-0.0040(4)	-0.0002(5)
C(125)	0.1835(4)	-0.5482(6)	-0.0936(6)	0.0066(4)	0.0116(7)	0.0119(7)	0.0047(4)	-0.0039(4)	-0.0025(6)
C(126)	0.2014(4)	-0.4556(5)	0.0023(6)	0.0046(3)	0.0096(6)	0.0103(6)	0.0028(3)	-0.0030(4)	-0.0002(5)
C(131)	0.1105(3)	-0.2897(5)	0.3155(5)	0.0034(2)	0.0083(5)	0.0080(5)	0.0021(3)	-0.0011(3)	0.0025(4)
C(132)	0.0483(4)	-0.3856(6)	0.3043(6)	0.0046(3)	0.0106(7)	0.0099(6)	0.0001(4)	-0.0013(4)	0.0028(5)
C(133)	-0.0093(4)	-0.4109(7)	0.4058(6)	0.0050(3)	0.0148(9)	0.0112(7)	-0.0011(4)	-0.0004(4)	0.0047(7)
C(134)	-0.0060(4)	-0.3432(7)	0.5174(6)	0.0060(4)	0.0151(9)	0.0115(8)	0.0029(5)	0.0009(4)	0.0057(7)
C(135)	0.0554(5)	-0.2492(6)	0.5297(6)	0.0075(4)	0.0122(7)	0.0075(6)	0.0026(5)	-0.0015(4)	0.0023(5)
C(136)	0.1127(4)	-0.2234(6)	0.4307(5)	0.0052(3)	0.0107(6)	0.0083(6)	0.0017(4)	-0.0018(3)	0.0028(5)
C(211)	0.2200(3)	0.1212(4)	-0.1932(4)	0.0026(2)	0.0064(4)	0.0067(4)	0.0015(2)	-0.0016(2)	0.0003(4)
C(212)	0.1474(3)	0.0582(5)	-0.1479(5)	0.0025(2)	0.0074(5)	0.0116(6)	0.0015(3)	-0.0016(3)	0.0023(4)
C(213)	0.0931(3)	0.0476(5)	-0.1884(6)	0.0029(2)	0.0112(6)	0.0135(7)	0.0020(3)	-0.0028(3)	0.0023(6)
C(214)	0.1117(4)	0.0997(6)	-0.2745(6)	0.0043(3)	0.0145(8)	0.0120(7)	0.0037(4)	-0.0042(4)	0.0003(6)
C(215)	0.1825(4)	0.1647(6)	-0.3197(5)	0.0049(3)	0.0139(7)	0.0089(6)	0.0039(4)	-0.0031(3)	0.0015(5)
C(216)	0.2372(3)	0.1762(5)	-0.2806(5)	0.0038(2)	0.0113(6)	0.0078(5)	0.0021(3)	-0.0019(3)	0.0027(5)
C(221)	0.3629(3)	0.2623(4)	-0.1781(5)	0.0024(2)	0.0065(4)	0.0089(5)	0.0010(2)	-0.0022(3)	0.0023(4)
C(222)	0.3456(4)	0.3677(5)	-0.1063(5)	0.0047(3)	0.0067(5)	0.0103(6)	0.0018(3)	-0.0016(3)	0.0012(5)
C(223)	0.3970(4)	0.4759(5)	-0.1194(6)	0.0065(4)	0.0061(5)	0.0133(8)	0.0008(3)	-0.0038(4)	0.0023(5)
C(224)	0.4657(4)	0.4801(6)	-0.2029(7)	0.0045(3)	0.0090(6)	0.0195(10)	-0.0014(3)	-0.0053(5)	0.0073(6)
C(225)	0.4816(4)	0.3794(6)	-0.2713(8)	0.0029(2)	0.0125(8)	0.0254(12)	0.0006(4)	-0.0018(5)	0.0113(8)
C(226)	0.4301(3)	0.2696(5)	-0.2612(6)	0.0030(2)	0.0097(6)	0.0174(9)	0.0019(3)	-0.0006(4)	0.0070(6)
C(231)	0.3314(3)	0.0128(4)	-0.2821(5)	0.0030(2)	0.0068(5)	0.0082(5)	0.0017(3)	-0.0008(3)	0.0020(4)
C(232)	0.3038(4)	-0.0478(5)	-0.3788(5)	0.0038(3)	0.0103(6)	0.0097(6)	0.0026(3)	-0.0013(3)	0.0012(5)
C(233)	0.3354(4)	-0.1264(6)	-0.4763(6)	0.0066(4)	0.0123(8)	0.0098(7)	0.0046(5)	-0.0018(4)	-0.0019(6)
C(234)	0.3965(4)	-0.1425(6)	-0.4794(6)	0.0066(4)	0.0121(8)	0.0127(8)	0.0054(5)	-0.0002(5)	0.0005(6)
C(235)	0.4253(4)	-0.0849(6)	-0.3877(7)	0.0049(3)	0.0147(8)	0.0148(8)	0.0055(4)	0.0005(4)	0.0059(7)
C(236)	0.3920(3)	-0.0061(5)	-0.2869(5)	0.0036(2)	0.0096(6)	0.0099(6)	0.0028(3)	0.0000(3)	0.0046(5)
O(1S)	0.6878(5)	0.5636(6)	0.4469(7)	0.0120(5)	0.0222(10)	0.0283(12)	0.0005(6)	-0.0084(7)	0.0051(9)
C(1S)	0.5993(6)	0.6309(12)	0.4747(12)	0.0090(7)	0.0390(22)	0.0346(21)	-0.0032(10)	-0.0105(10)	0.0205(18)
C(2S)	0.6176(7)	0.5567(12)	0.5088(10)	0.0101(7)	0.0447(26)	0.0192(14)	-0.0109(11)	-0.0058(8)	0.0133(16)
C(3S)	0.7117(11)	0.4922(16)	0.4835(18)	0.0207(14)	0.0431(28)	0.0620(39)	0.0055(17)	-0.0158(20)	0.0299(27)
C(4S)	0.7812(8)	0.5266(17)	0.4604(14)	0.0113(9)	0.0605(34)	0.0330(23)	0.0132(15)	0.0012(12)	0.0193(23)

2.089 (5) Å, respectively] are in excellent agreement but are significantly shorter than Rh(1)–C(2) and Rh(2)–C(1) [2.121 (5) and 2.128 (5) Å, respectively], which, in turn, are also equal within experimental error. These differences indicate that the C≡C bond of the bridging acetylene group is not precisely normal to the Rh–Rh axis.

The Rh–Rh distance [2.740 (1) Å] is only slightly longer than the corresponding distances found in the metal (2.69 Å)[26] and in $(C_5H_5)_2Rh_2(CO)_3$ [2.681 (2) Å][27] and is taken to indicate the presence of a metal–metal bond. A similar Rh–Rh

Table Vb. Calculated Hydrogen Atom Coordinates and Fixed Isotropic Thermal Parameters for $Rh_2(PF_3)_4[P(C_6H_5)_3]_2(C_6H_5C_2C_6H_5)\cdot(C_2H_5)_2O$[a]

ATOM	X	Y	Z	B(A**2)	ATOM	X	Y	Z	B(A**2)
H(12)	0.056	-0.124	0.093	4.3	H(132)	0.046	-0.439	0.215	7.0
H(13)	-0.034	-0.233	-0.019	5.7	H(133)	-0.058	-0.486	0.396	9.0
H(14)	0.007	-0.326	-0.234	6.2	H(134)	-0.051	-0.364	0.596	8.7
H(15)	0.139	-0.311	-0.340	5.7	H(135)	0.058	-0.195	0.619	7.9
H(16)	0.229	-0.203	-0.227	4.3	H(136)	0.161	-0.149	0.441	6.3
H(22)	0.416	0.032	-0.014	5.1	H(212)	0.134	0.016	-0.080	4.7
H(23)	0.515	-0.061	-0.124	6.1	H(213)	0.036	-0.003	-0.152	5.9
H(24)	0.489	-0.268	-0.247	7.1	H(214)	0.069	0.091	-0.306	6.6
H(25)	0.363	-0.384	-0.259	6.4	H(215)	0.196	0.207	-0.387	6.2
H(26)	0.263	-0.291	-0.149	4.6	H(216)	0.294	0.227	-0.317	5.3
H(112)	0.343	-0.143	0.108	5.4	H(222)	0.291	0.363	-0.041	5.9
H(113)	0.448	-0.188	0.105	6.7	H(223)	0.384	0.558	-0.063	7.0
H(114)	0.424	-0.340	0.192	7.2	H(224)	0.506	0.565	-0.212	7.2
H(115)	0.299	-0.448	0.285	7.0	H(225)	0.536	0.384	-0.337	8.2
H(116)	0.192	-0.406	0.292	6.2	H(226)	0.443	0.188	-0.317	6.4
H(122)	0.081	-0.315	0.069	4.6	H(232)	0.256	-0.033	-0.375	5.9
H(123)	0.051	-0.479	-0.105	6.0	H(233)	0.313	-0.174	-0.551	8.0
H(124)	0.115	-0.628	-0.206	7.1	H(234)	0.422	-0.204	-0.557	8.4
H(125)	0.212	-0.614	-0.140	7.7	H(235)	0.473	-0.099	-0.391	7.6
H(126)	0.244	-0.449	0.032	5.9	H(236)	0.414	0.041	-0.213	5.3

[a] Hydrogen atoms are numbered according to the carbon atoms to which they are bonded.

Table VI. Principal Bond Distances and Interbond Angles for $Rh_2(PF_3)_4[P(C_6H_5)_3]_2(C_6H_5C_2C_6H_5)\cdot(C_2H_5)_2O$

Atoms	*m* = 1	*m* = 2	Atoms	*m* = 1	*m* = 2
		(a) Bond Distances, Å			
Rh(1)-Rh(2)	2.740 (1)		C(1)-C(2)	1.369 (7)	
Rh(*m*)-P(*m*0)	2.388 (1)	2.389 (1)	Rh(*m*)-P(*m*1)	2.227 (2)	2.217 (2)
Rh(*m*)-P(*m*2)	2.211 (1)	2.222 (2)	Rh(*m*)-C(*m*)	2.079 (5)	2.089 (5)
Rh(*m*)-C(2)	2.121 (5)		Rh(*m*)-C(1)		2.128 (5)
P(*m*0)-C(*m*11)	1.829 (6)	1.821 (5)	P(*m*0)-C(*m*21)	1.831 (5)	1.842 (5)
P(*m*0)-C(*m*31)	1.827 (6)	1.828 (5)	P(*m*1)-F(*m*11)	1.553 (4)	1.539 (4)
P(*m*1)-F(*m*12)	1.533 (4)	1.547 (4)	P(*m*1)-F(*m*13)	1.527 (4)	1.550 (5)
P(*m*2)-F(*m*21)	1.555 (4)	1.505 (4)	P(*m*2)-F(*m*22)	1.545 (4)	1.518 (6)
P(*m*2)-F(*m*23)	1.552 (4)	1.543 (4)	C(*m*)-C(*m*1)	1.459 (7)	1.460 (7)
C(*m*1)-C(*m*2)	1.394 (7)	1.407 (8)	C(*m*2)-C(*m*3)	1.390 (8)	1.370 (8)
C(*m*3)-C(*m*4)	1.371 (9)	1.387 (10)	C(*m*4)-C(*m*5)	1.388 (9)	1.379 (10)
C(*m*5)-C(*m*6)	1.391 (8)	1.392 (9)	C(*m*6)-C(*m*1)	1.394 (7)	1.391 (7)
O(1S)-C(2S)	1.33 (2)		O(1S)-C(3S)	1.52 (2)	
C(1S)-C(2S)	1.44 (2)		C(3S)-C(4S)	1.27 (3)	
		(b) Interbond Angles, Deg			
Rh(2)-Rh(1)-P(10)	149.01 (4)		Rh(1)-Rh(2)-P(20)	148.48 (4)	
Rh(2)-Rh(1)-P(11)	108.13 (4)		Rh(1)-Rh(2)-P(21)	101.25 (4)	
Rh(2)-Rh(1)-P(12)	100.73 (4)		Rh(1)-Rh(2)-P(22)	107.78 (4)	
Rh(2)-Rh(1)-C(1)	50.1 (1)		Rh(1)-Rh(2)-C(1)	49.1 (1)	
Rh(2)-Rh(1)-C(2)	48.9 (1)		Rh(1)-Rh(2)-C(2)	49.9 (1)	
C(1)-Rh(1)-C(2)	37.9 (2)		C(1)-Rh(2)-C(2)	37.9 (2)	
P(*m*0)-Rh(*m*)-P(*m*1)	95.81 (5)	96.49 (5)	P(*m*0)-Rh(*m*)-P(*m*2)	95.36 (5)	95.16 (5)
P(*m*1)-Rh(*m*)-P(*m*2)	97.14 (6)	98.00 (6)	Rh(*m*)-P(*m*0)-C(*m*11)	117.4 (2)	117.5 (2)
Rh(*m*)-P(*m*0)-C(*m*21)	115.7 (2)	115.4 (2)	Rh(*m*)-P(*m*0)-C(*m*31)	115.0 (2)	116.3 (2)
C(*m*11)-P(*m*0)-C(*m*21)	101.8 (2)	101.4 (2)	C(*m*11)-P(*m*0)-C(*m*31)	101.6 (2)	102.0 (2)
C(*m*21)-P(*m*0)-C(*m*31)	103.2 (2)	101.9 (2)	Rh(*m*)-P(*m*1)-F(*m*11)	120.5 (2)	118.7 (2)
Rh(*m*)-P(*m*1)-F(*m*12)	122.7 (2)	123.3 (2)	Rh(*m*)-P(*m*1)-F(*m*13)	120.7 (2)	121.7 (2)
F(*m*11)-P(*m*1)-F(*m*12)	93.2 (3)	96.1 (2)	F(*m*11)-P(*m*1)-F(*m*13)	95.3 (3)	95.6 (2)
F(*m*12)-P(*m*1)-F(*m*13)	97.7 (3)	94.9 (2)	Rh(*m*)-P(*m*2)-F(*m*21)	121.6 (2)	121.5 (3)
Rh(*m*)-P(*m*2)-F(*m*22)	117.7 (2)	124.0 (2)	Rh(*m*)-P(*m*2)-F(*m*23)	123.4 (2)	120.8 (2)
F(*m*21)-P(*m*2)-F(*m*22)	95.8 (2)	96.7 (3)	F(*m*21)-P(*m*2)-F(*m*23)	94.7 (2)	93.8 (3)
F(*m*22)-P(*m*2)-F(*m*23)	97.4 (2)	92.4 (2)			
C(2)-C(1)-C(11)	141.1 (5)		C(1)-C(2)-C(21)	141.5 (5)	
C(*m*)-C(*m*1)-C(*m*2)	121.0 (4)	121.2 (4)	C(*m*)-C(*m*1)-C(*m*6)	120.5 (5)	120.6 (4)
C(*m*2)-C(*m*1)-C(*m*6)	118.4 (5)	118.1 (5)	C(*m*1)-C(*m*2)-C(*m*3)	120.8 (5)	121.2 (5)
C(*m*2)-C(*m*3)-C(*m*4)	120.1 (5)	119.9 (6)	C(*m*3)-C(*m*4)-C(*m*5)	120.4 (6)	120.1 (6)
C(*m*4)-C(*m*5)-C(*m*6)	119.6 (5)	120.1 (6)	C(*m*5)-C(*m*6)-C(*m*1)	120.7 (5)	120.5 (5)
C(2S)-O(1S)-C(3S)	109 (1)		C(1S)-C(2S)-O(1S)	107 (1)	
O(1S)-C(3S)-C(4S)	111 (1)				

distance (average 2.73 Å) has been observed for $Rh_4(CO)_{12}$.[28] The configuration about the rhodium–rhodium axis is not precisely eclipsed (see Table IX). The torsion angles between the PF_3 phosphorus atoms average 9.0°, but the torsion angle between P(10) and P(20) is 24.3°. The increased staggering of the triphenylphosphine groups in the solid state is most probably a consequence of the fact that the triphenylphosphine groups and the bridging diphenylacetylene group are on the same "side" of the molecule.

The Rh–P(PF_3) distances (average 2.219 Å) are significantly shorter than the Rh–P[$P(C_6H_5)_3$] distances (average 2.388 Å), probably reflecting the increased π-bonding ability of PF_3 as a ligand relative to $P(C_6H_5)_3$.

The P–F distances [range 1.505 (4)–1.555 (4) Å; average 1.539 Å] are considerably shorter than those found for free PF_3 [1.569 (1) Å by electron diffraction].[29] Similar P–F bond length contractions have been observed for $PF_3\cdot BH_3$[30] and $Pt(PF_3)_4$[31] and have been attributed to σ-electron donation

Table VII. Bond Distances and Interbond Angles within the Triphenylphosphine Phenyl Rings of $Rh_2(PF_3)_4[P(C_6H_5)_3]_2(C_6H_5C_2C_6H_5)\cdot(C_2H_5)_2O$

Atoms	$m = 1, n = 1$	$m = 1, n = 2$	$m = 1, n = 3$	$m = 2, n = 1$	$m = 2, n = 2$	$m = 2, n = 3$
			(a) Bond Distances, Å			
P(*m*0)–C(*mn*1)	1.829 (6)	1.831 (5)	1.826 (6)	1.821 (5)	1.842 (5)	1.828 (5)
C(*mn*1)–C(*mn*2)	1.387 (8)	1.403 (8)	1.387 (9)	1.385 (7)	1.403 (8)	1.401 (8)
C(*mn*2)–C(*mn*3)	1.389 (9)	1.392 (8)	1.396 (10)	1.395 (8)	1.384 (9)	1.373 (9)
C(*mn*3)–C(*mn*4)	1.349 (10)	1.368 (9)	1.364 (10)	1.364 (9)	1.382 (10)	1.378 (11)
C(*mn*4)–C(*mn*5)	1.348 (10)	1.375 (11)	1.368 (11)	1.366 (10)	1.334 (10)	1.361 (10)
C(*mn*5)–C(*mn*6)	1.412 (10)	1.389 (9)	1.373 (9)	1.387 (9)	1.393 (9)	1.406 (9)
C(*mn*6)–C(*mn*1)	1.400 (8)	1.372 (8)	1.393 (8)	1.415 (7)	1.355 (8)	1.378 (8)
			(b) Interbond Angles, Deg			
P(*m*0)–C(*mn*1)–C(*mn*2)	119.2 (4)	118.0 (4)	122.9 (4)	121.3 (4)	117.8 (4)	122.3 (4)
P(*m*0)–C(*mn*1)–C(*mn*6)	121.4 (4)	123.3 (4)	119.9 (4)	120.6 (4)	123.9 (5)	118.8 (4)
C(*mn*2)–C(*mn*1)–C(*mn*6)	118.9 (5)	118.7 (5)	117.2 (5)	117.8 (5)	118.3 (5)	118.9 (5)
C(*mn*1)–C(*mn*2)–C(*mn*3)	120.1 (6)	120.3 (5)	120.0 (6)	121.1 (5)	120.3 (6)	121.0 (6)
C(*mn*2)–C(*mn*3)–C(*mn*4)	120.9 (6)	119.7 (6)	121.4 (7)	119.7 (6)	119.8 (6)	118.9 (6)
C(*mn*3)–C(*mn*4)–C(*mn*5)	120.5 (7)	120.6 (6)	119.2 (7)	121.0 (6)	119.5 (6)	122.0 (7)
C(*mn*4)–C(*mn*5)–C(*mn*6)	120.9 (6)	119.9 (6)	120.2 (7)	120.1 (6)	121.5 (7)	119.0 (6)
C(*mn*1)–C(*mn*6)–C(*mn*5)	118.6 (6)	120.9 (6)	122.1 (7)	120.2 (5)	120.5 (7)	120.2 (6)

Table VIII. Least-Squares Planes within $Rh_2(PF_3)_4[P(C_6H_5)_3]_2(C_6H_5C_2C_6H_5)\cdot(C_2H_5)_2O$

(a) Best Weighted Least-Squares Planes

Plane	Atoms defining plane	Equation[a]
1	C(11)–C(16) phenyl ring	$-0.3229X + 0.9288Y - 0.1820Z + 2.5947 = 0$
2	C(21)–C(26) phenyl ring	$-0.2881X + 0.5446Y - 0.7877Z + 2.1174 = 0$
3	C(111)–C(116) phenyl ring	$-0.1184X - 0.4685Y - 0.8755Z + 1.1441 = 0$
4	C(121)–C(126) phenyl ring	$0.2144X + 0.7536Y - 0.6214Z + 2.5941 = 0$
5	C(131)–C(136) phenyl ring	$-0.7841X + 0.6206Y - 0.0118Z + 7.2699 = 0$
6	C(211)–C(216) phenyl ring	$0.2436X - 0.6557Y - 0.7146Z - 0.9120 = 0$
7	C(221)–C(226) phenyl ring	$-0.7209X + 0.1562Y - 0.6752Z + 1.8450 = 0$
8	C(231)–C(236) phenyl ring	$0.1174X + 0.8974Y - 0.4253Z - 2.9223 = 0$

(b) Deviations of Atoms from Best Planes, Å

Atom	Plane 1	Atom	Plane 1	Atom	Plane 2	Atom	Plane 2
C(11)	−0.002 (5)	C(16)	−0.003 (6)	C(21)	0.002 (5)	C(26)	0.002 (6)
C(12)	0.005 (6)	C(1)	0.053 (5)	C(22)	−0.003 (6)	C(1)	0.110 (5)
C(13)	−0.004 (7)	C(2)	−0.114 (5)	C(23)	0.000 (7)	C(2)	−0.031 (5)
C(14)	−0.004 (7)	C(21)	−0.741 (5)	C(24)	0.005 (7)	C(11)	0.683 (5)
C(15)	0.007 (6)			C(25)	−0.006 (7)		

Atom	Plane 3 $m = 1, n = 1$	Plane 4 $m = 1, n = 2$	Plane 5 $m = 1, n = 3$	Plane 6 $m = 2, n = 1$	Plane 7 $m = 2, n = 2$	Plane 8 $m = 2, n = 3$
C(*mn*1)	−0.005 (5)	0.004 (5)	0.006 (7)	0.007 (5)	−0.008 (6)	−0.001 (6)
C(*mn*2)	0.009 (6)	−0.009 (6)	−0.004 (8)	−0.005 (6)	0.002 (8)	0.008 (7)
C(*mn*3)	−0.007 (7)	0.010 (7)	−0.002 (10)	−0.004 (7)	0.008 (9)	−0.011 (7)
C(*mn*4)	−0.002 (7)	−0.002 (7)	0.005 (10)	0.012 (7)	−0.006 (9)	0.004 (8)
C(*mn*5)	0.006 (7)	−0.005 (7)	0.001 (10)	−0.006 (7)	−0.008 (9)	0.004 (8)
C(*mn*6)	0.000 (7)	0.001 (6)	−0.006 (8)	−0.005 (6)	0.015 (8)	−0.003 (6)
P(*m*0)	0.183 (1)	0.021 (1)	0.080 (2)	0.193 (1)	−0.059 (2)	0.079 (1)

[a] The equations of the planes $LX + MY + NZ + D = 0$ refer to orthogonal coordinates. The equations to transform from triclinic (fractional) to orthogonal (angstrom) coordinates are $X = 21.1861x - 5.5590y + 5.6000z$, $Y = 0.0x + 11.7452y - 3.1993z$, and $Z = 0.0x + 0.0y + 11.2205z$.

Table IX. Some Important Torsion Angles for $Rh_2(PF_3)_4[P(C_6H_5)_3]_2(C_6H_5C_2C_6H_5)\cdot(C_2H_5)_2O$

Axis atoms	Atom 1	Atom 2	Torsion angle,[a] deg
Rh(1), Rh(2)	P(10)	P(20)	24.27
Rh(1), Rh(2)	P(11)	P(21)	8.52
Rh(1), Rh(2)	P(12)	P(22)	9.52
C(1), C(2)	C(11)	C(21)	20.58

[a] The torsion angle is defined as the dihedral angle between the two three-atom planes [axis atoms, atom 1] and [axis atoms, atom 2].

from the ligand to the metal.[31] The F–P–F angles are significantly less than the tetrahedral angle (average 95.3°) and are in good agreement with values of 97.7 (2) and 98.9 (7)° found for the corresponding angles in PF_3[29] and $Pt(PF_3)_4$,[31] respectively.

Although the geometry of the solvent ether molecule is far from ideal, there is no evidence of disorder. There are no unusually short contacts between the solvent ether molecule and molecules of $Rh_2(PF_3)_4[P(C_6H_5)_3]_2(C_6H_5C_2C_6H_5)$.

Spectroscopic Properties and Fluxional Behavior. The bis(monodentate ligand) complexes of symmetrically disubstituted acetylenes, $Rh_2(PF_3)_4L_2(RC_2R)$, show one doublet of ca. 1400-Hz separation due to P–F coupling ($^1J_{PF} + {}^3J_{PF}$) in their room-temperature ^{19}F NMR spectra, whereas the complexes of unsymmetrical acetylenes show two such doublets in their low-temperature limiting spectra (Table X). These observations suggest that the complexes are all structurally similar to $Rh_2(PF_3)_4[P(C_6H_5)_3]_2(C_6H_5C_2C_6H_5)$ and that in solution they possess the time-averaged eclipsed structure shown in the form of a Newman projection along the Rh–Rh bond in Figure 4. In this structure, the PF_3 groups are all equivalent when R = R' and fall into two inequivalent pairs when R ≠ R'. We emphasize that this structure is time averaged since, as noted previously, the triphenylphosphine

Table X. ^{19}F NMR Data^a

Compd	ϕ_F (multiplicity, "J_{PF}")
$Rh_2(PF_3)_4[P(C_6H_5)_3]_2(C_6H_5C_2C_6H_5)$	5.58 (d, 1390)
$Rh_2(PF_3)_4[P(CH_3)(C_6H_5)_2]_2(C_6H_5C_2C_6H_5)$	5.75 (d, 1385)
$Rh_2(PF_3)_4[As(C_6H_5)_3]_2(C_6H_5C_2C_6H_5)$	5.68 (d, 1385)
$Rh_2(PF_3)_4[P(C_6H_5)_3]_2(C_6H_5C_2CH_3)$	4.35 (d, 1360), 5.69 (d, 1380)
$Rh_2(PF_3)_4[P(CH_3)(C_6H_5)_2]_2(C_6H_5C_2CH_3)$	4.62 (d, 1360), 5.78 (d, 1385)
$Rh_2(PF_3)_4[P(CH_3)(C_6H_5)_2]_2(C_6H_5C_2CH_3)^b$	3.22 (d, 1410)
$Rh_2(PF_3)_4[As(C_6H_5)_3]_2(C_6H_5C_2CH_3)$	5.51 (d, 1385)
$Rh_2(PF_3)_4[As(C_6H_5)_3]_2(C_6H_5C_2CH_3)^c$	4.00 (d, 1360), 5.24 (d, 1390)
$Rh_2(PF_3)_4[As(CH_3)(C_6H_5)_2]_2(C_6H_5C_2CH_3)^d$	4.83 (d, 1365), 5.79 (d, 1385)
$Rh_2(PF_3)_4[As(CH_3)(C_6H_5)_2]_2(C_6H_5C_2CH_3)^e$	5.41 (d, 1385)
$Rh_2(PF_3)_4[As(C_6H_5)_3]_2(p\text{-}NO_2C_6H_4C_2CO_2C_2H_5)^d$	4.41 (d, 1385), 6.11 (d, 1405)
$Rh_2(PF_3)_4[As(C_6H_5)_3]_2(p\text{-}NO_2C_6H_4C_2CO_2C_2H_5)^f$	5.79 (d, 1415)
$Rh_2(PF_3)_2(diars)_2(C_6H_5C_2C_6H_5)^g$	−0.19 (dd, 1375)^i
$Rh_2(PF_3)_2(diars)_2(C_6H_5C_2CH_3)^h$	0.20 (dd, 1360)^i

^{a} Chemical shifts (ϕ_F) in ppm upfield of internal $CFCl_3$ measured in toluene at +24° except where indicated. "J_{PF}" (in Hz) = $|^1J_{PF} + {}^3J_{PF}|$ and is believed accurate to ±10 Hz. Abbreviations: d, doublet; dd, doublet of doublets. ^{b} In toluene at 110°. ^{c} In THF at −30°. ^{d} In C_6H_5F at 24°. ^{e} In C_6H_5F at 55°. ^{f} In C_6H_5F at 85°. ^{g} J_{RhF} = 23 ± 2 Hz; spectrum similar at −77°. ^{h} J_{RhF} = 21 ± 2 Hz; spectrum similar at −91°. ^{i} "J_{PF}" = $^1J_{PF}$.

Table XI. Free Energy of Activation for Intramolecular Exchange of Trifluorophosphine in Complexes $Rh_2(PF_3)_4L_2(RC_2R')^a$

Compd	Solvent	Temp, °C	Rates, sec^{-1}	$\Delta G^\ddagger$, kcal/mol
$Rh_2(PF_3)_4[As(C_6H_5)_3]_2(C_6H_5C_2CH_3)$	Toluene	−16–+12	20–400	13.5 ± 0.3
$Rh_2(PF_3)_4[As(CH_3)(C_6H_5)_2]_2(C_6H_5C_2CH_3)$	Fluorobenzene	28–44	20–80	15.8 ± 0.5
$Rh_2(PF_3)_4[P(CH_3)(C_6H_5)_2]_2(C_6H_5C_2CH_3)$	*p*-Xylene	69–100	40–300	17.9 ± 0.5
$Rh_2(PF_3)_4[P(C_6H_5)_3]_2(C_6H_5C_2CH_3)$	Toluene	30^b	<20	>16
$Rh_2(PF_3)_4[As(C_6H_5)_3]_2(p\text{-}O_2NC_6H_4C_2CO_2C_2H_5)$	Fluorobenzene	62–80	60–500	16.9 ± 0.5

^{a} Rates were estimated by comparison of ^{19}F NMR spectra with calculated line shapes over temperature range given. $\Delta G^\ddagger$ in the table was a mean of values obtained over the range and none fell outside the range indicated by the estimated error. ^{b} The instability in solution at higher temperatures together with poor solubility prevented observation of intramolecular exchange of PF_3.

Table XII. ^{1}H NMR Data^a

Compd	δ (multiplicity, J_{P,CH_3})	
	Acetylenic methyl groups	Ligand methyl groups
$Rh_2(PF_3)_4[P(CH_3)(C_6H_5)_2]_2(C_6H_5C_2C_6H_5)$		1.42 (d, 7)
$Rh_2(PF_3)_4[P(C_6H_5)_3]_2(C_6H_5C_2CH_3)$	2.18 (t, br, 14)	
$Rh_2(PF_3)_4[As(C_6H_5)_3]_2(C_6H_5C_2CH_3)^b$	2.20 (qn, br, 7)	
$Rh_2(PF_3)_4[P(CH_3)(C_6H_5)_2]_2(C_6H_5C_2CH_3)$	1.57 (t, br, 17)	1.50 (d, 7)
$Rh_2(PF_3)_4[As(CH_3)(C_6H_5)_2]_2(C_6H_5C_2CH_3)^c$	2.20 (qn, br, 7)	1.57 (s)
$Rh_2(PF_3)_4[As(CH_3)(C_6H_5)_2]_2(C_6H_5C_2CH_3)^d$	1.89 (t, br, 16)	1.34 (s, br)
$Rh_2(PF_3)_4[P(C_6H_5)_3]_2(CH_3C_2CH_3)^e$	1.89 (t, br, 14)	
$Rh_2(PF_3)_4[As(C_6H_5)_3]_2(p\text{-}NO_2C_6H_4C_2CO_2C_2H_5)^f$	1.10 (t), 3.94 (q)^g	
$Rh_2(PF_3)_2(diars)_2(C_6H_5C_2C_6H_5)$		1.14 (s), 1.58 (s)
$Rh_2(PF_3)_2(diars)_2(C_6H_5C_2CH_3)$	2.81 (t, br, 8)	1.18 (s), 1.32 (s), 1.50 (s), 1.56 (s)

^{a} Chemical shifts (δ) in ppm downfield of internal TMS, measured in C_6D_6 at 32° except where indicated. Coupling constants (J) are in Hz. Abbreviations: s, singlet; t, triplet; q, quartet; qn, quintet; br, broad. All aromatic signals are in the normal range δ 6.5–8.0. ^{b} In $CHCl_3$. ^{c} In C_6H_5F at +59°. ^{d} In C_6H_5F at −4°. ^{e} Not isolated in a pure state. ^{f} In C_6H_5F. ^{g} Ethyl resonances; $J_{CH_2-CH_3}$ = 7 Hz.

groups of $Rh_2(PF_3)_4[P(C_6H_5)_3]_2(C_6H_5C_2C_6H_5)$ are appreciably staggered in the solid state. It may of course be that the resulting inequivalence of PF_3 groups is too small to be observed by ^{19}F NMR in solution, but it seems more likely that there is a low-energy process which averages the position of the triphenylphosphine groups in the eclipsed conformation.

On raising the temperature, the signals of the inequivalent PF_3 groups in the unsymmetrical acetylene complexes broaden, coalesce, and finally sharpen again to give one doublet. This change occurs between 70 and 100° in the case of $Rh_2(PF_3)_4[P(CH_3)(C_6H_5)_2]_2(C_6H_5C_2CH_3)$, but in the analogous tertiary arsine derivatives it takes place at appreciably lower temperatures (Table XI). The triphenylphosphine derivative is rigid at 40° but unfortunately undergoes irreversible decomposition above this temperature; ^{19}F NMR spectroscopy showed that even at 24° about 15% of $Rh_2(PF_3)_6(C_6H_5C_2CH_3)$ had been formed after 12 hr. The process responsible for the coalescence behavior is reversible and arises from intramolecular rather than intermolecular exchange of PF_3, since the high-temperature spectra contain fine structure attributable to the complex spin system of $Rh(PF_3)_2$. Approximate line-shape analysis[1] of several of these spectra gave the rates and free energies of activation ($\Delta G^\ddagger$) shown in Table XI. It is qualitatively evident from the temperature ranges and quantitatively confirmed by the $\Delta G^\ddagger$ values that the barrier to PF_3 rearrangement is higher for the tertiary phosphine derivatives than for the tertiary arsine derivatives. This suggests that the intramolecular rearrangement of PF_3 groups may be intimately associated with intermolecular exchange of the phosphine or arsine; tertiary arsines are generally more weakly bound and are more labile than tertiary phosphines,

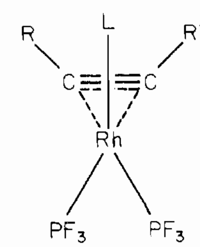

Figure 4. Proposed time-averaged structure of $Rh_2(PF_3)_4L_2(RC_2R')$ viewed along the Rh–Rh axis. A second $Rh(PF_3)_2L$ group is behind and eclipses the one shown.

as is evident from their exchange behavior with π-allylic palladium(II) complexes and dienerhodium(I) complexes.[32]

Evidence for ligand exchange also comes from ^1H NMR spectra (Table XII). In the triphenylarsine complex of 1-phenylpropyne ($C_6H_5C_2CH_3$), the acetylenic methyl resonance appears as a quintet at 34° as a result of coupling with four apparently equivalent ^{31}P nuclei of coordinated PF_3 (J = 7 Hz); there is also some broadening due to coupling with ^{19}F. This suggests rapid exchange at 34° which renders all the PF_3 groups equivalent. The same behavior is observed for the analogous diphenylmethylarsine complex at 59°. In the analogous tertiary phosphine complexes the acetylenic methyl resonance appears as a broad triplet (J = 14 Hz), as a consequence of coupling to *two* equivalent ^{31}P nuclei of one pair of trifluorophosphine ligands (cf. the arsine complex below), so that these complexes cannot be undergoing rapid exchange on the NMR time scale at 34°. The broadening probably arises from smaller couplings to the ^{31}P nuclei of the other pair of PF_3 groups and of the pair of $P(C_6H_5)_3$ groups, and possibly also to ^{19}F nuclei. At lower temperatures (−4°) the acetylenic methyl resonance of $Rh_2(PF_3)_4[As(CH_3)(C_6H_5)_2]_2(C_6H_5C_2CH_3)$ also becomes a triplet (J = 16 Hz), showing that exchange is now slow on the NMR time scale; this corresponds to the situation found for the phosphine complexes at 34°. The triplet of the diphenylmethylarsine complex is sharper than that of the tertiary phosphine complexes, presumably because one source of coupling is absent. Addition of free diphenylmethylarsine to the solution at −4° gives a separate methyl resonance for this species, showing clearly that intermolecular exchange of the arsine is slow at this temperature, but, on warming, the resonances of free and coordinated diphenylmethylarsine coalesce and become a sharp singlet owing to rapid intermolecular exchange of the tertiary arsine. The temperature at which the sharp singlet is observed for the methyl resonance of diphenylmethylarsine is about the same (ca. +59°) as that at which a clear quintet is observed for the acetylenic methyl resonance as a result of intramolecular PF_3 exchange (see above). Unfortunately it proved impossible to measure the barrier to intermolecular exchange owing to the large temperature dependence of the chemical shifts of both the free and coordinated arsenic methyl resonance; e.g., for solutions in fluorobenzene with TMS as internal reference free diphenylmethylarsine has δ_{CH_3} 1.29 at 30° and 1.42 at −4°, and coordinated diphenylmethylarsine in $Rh_2(PF_3)_4[As(CH_3)(C_6H_5)_2]_2(C_6H_5C_2CH_3)$ has δ_{CH_3} 1.57 at 59° and 1.34 at −4°. Qualitatively, however, the intermolecular exchange of diphenylmethylarsine in $Rh_2(PF_3)_4[As(CH_3)(C_6H_5)_2]_2(C_6H_5C_2CH_3)$ occurs over the same temperature range as intramolecular PF_3 exchange, and a rough estimate of the intramolecular exchange, based on the change from a triplet to a quintet in the acetylenic methyl resonance, gives a barrier in reasonable agreement with that derived from ^{19}F NMR. We assume therefore, that the intermolecular exchange process triggers the intramolecular process. Addition of free tertiary phosphine or arsine to the respective complexes had no effect on the rate of intramolecular exchange, showing that the rate-determining step is the loss of phosphine or arsine. The effect of solvent appears to be negligible, since the variable-temperature ^{19}F NMR spectra of $Rh_2(PF_3)_4[As(C_6H_5)_3]_2(C_6H_5C_2CH_3)$ in toluene and in tetrahydrofuran were indistinguishable. Changes in concentration by a factor of 2 also had no effect on the rates.

Dissociation of one ligand molecule from $Rh_2(PF_3)_4L_2(RC_2R')$ should give a coordinately unsaturated species $Rh_2(PF_3)_4L(RC_2R')$, and we require a mechanism which will interchange the PF_3 groups of the $Rh(PF_3)_2$ moiety in this intermediate either before or during reentry of ligand. Since

Scheme I

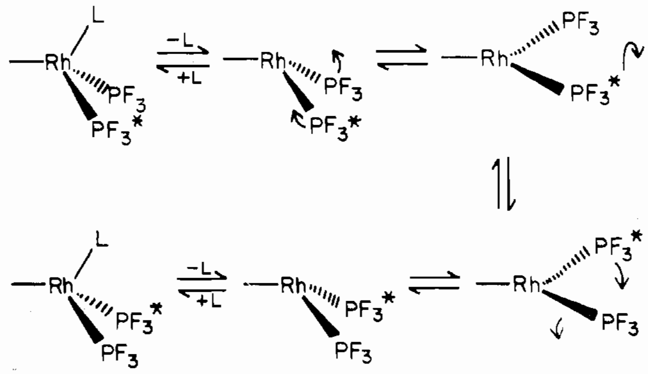

ligand dissociation can occur at either end of the initial molecule, any such process will average all the PF_3 environments. One possibility consists of a bending mode which brings the two PF_3 groups into the plane of the metal–metal bond, followed by a 180° rotation about the Rh–Rh axis, and another bend to bring the PF_3 groups to their interchanged positions (Scheme I). This process is assumed to be fast relative to ligand dissociation. Rotation of PF_3 groups about the metal–metal bond has also been proposed to account for the behavior of the di-*tert*-butylacetylene complex $Rh_2(PF_3)_5(t\text{-}Bu_2C_2)$,[33] which is a stable analogue of the coordinately unsaturated intermediate proposed herein; to this complex the rhodium–rhodium double-bonded structure I has

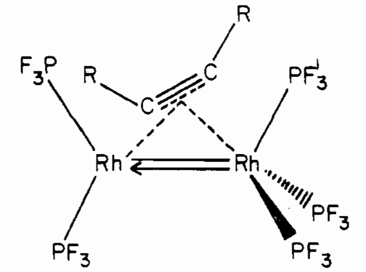

I(R = *t*-Bu)

been assigned. In this complex, the signals of the inequivalent PF_3 groups of the $Rh(PF_3)_2$ moiety coalesce on warming from 24 to 110°, as do those of the $Rh(PF_3)_3$ moiety. The free energies of activation for the two processes are identical, and it seems reasonable to assume that the PF_3 groups rotate about the metal–metal bond. A somewhat different explanation for the PF_3 exchange in $Rh_2(PF_3)_4L(RC_2R')$ is to assume that this intermediate has the same stereochemistry as $Rh_2(PF_3)_5(t\text{-}Bu_2C_2)$ (structure I). Ligand L can then recombine with the intermediate from either side of the molecule, leading to exchange of the PF_3 groups. This explanation raises the possibility that intramolecular PF_3 exchange might be inhibited if R and R' were sterically very different, since L might prefer to recombine on the same side from which it left. Attempts to obtain a pure sample of $Rh_2(PF_3)_4[As(C_6H_5)_3]_2(t\text{-}BuC_2H)$ to test this hypothesis were not successful. A third possible explanation involves dissociation of both ligand molecules from $Rh_2(PF_3)_4L_2(RC_2R')$ to give an intermediate $Rh_2(PF_3)_4(RC_2R')$ in which the acetylene can rotate rapidly about an axis bisecting the Rh–Rh bond, so that the PF_3 environments are averaged. The available data are insufficient to distinguish between these possibilities, though we favor either of the first two given above in view of the isolation and fluxional behavior of $Rh_2(PF_3)_5(t\text{-}Bu_2C_2)$.[33] Comparison of the $\Delta G^{\ddagger}$ values for $Rh_2(PF_3)_4[As(C_6H_5)_3]_2(C_6H_5C_2CH_3)$ and for $Rh_2(PF_3)_4[As(C_6H_5)_3]_2(p\text{-}NO_2C_6H_4C_2CO_2C_2H_5)$ shows that the more electron-withdrawing acetylene gives rise to the higher barrier to intramolecular PF_3 exchange, as was also found for the

$Rh_2(PF_3)_6$(ac) complexes.[1] In the bis(ligand) complexes, however, this electronic effect may well be exerted directly on the rate of ligand dissociation rather than on the rate of intramolecular PF_3 exchange. The fact that pairwise PF_3 exchange is probably initiated by dissociation of tertiary phosphine or arsine suggests (though it does not prove) that such pairwise PF_3 exchange does not occur in the $Rh_2(PF_3)_6$(ac) complexes.

Intermolecular PF_3 Exchange. The ^{19}F NMR spectrum of a 1:1 mixture of $Rh_2(PF_3)_4[P(C_6H_5)_3]_2(C_6H_5C_2C_6H_5)$ and $Rh_2(PF_3)_6(C_6H_5C_2C_6H_5)$ at room temperature consists of the two doublets, intensity ratio 2:3, characteristic of each compound. On cooling, the upfield doublet due to the latter complex broadens and separates into two peaks, as observed for the pure compound,[1] while the low-field doublet remains unchanged. This behavior suggests that the two complexes do not react to form $Rh_2(PF_3)_5[P(C_6H_5)_3](C_6H_5C_2C_6H_5)$ at or below room temperature.

A 1:1 mixture of $Rh_2(PF_3)_4[As(CH_3)(C_6H_5)_2]_2(C_6H_5C_2CH_3)$ and $Rh_2(PF_3)_6(C_6H_5C_2CH_3)$ in fluorobenzene also exhibits a room-temperature ^{19}F NMR spectrum characteristic of each complex, i.e., a pair of doublets for the former and one doublet about 3 ppm to higher field for the latter. At higher temperatures (~45°) the pair of doublets coalesce owing to the intramolecular PF_3 exchange already discussed. In the range 50–82° the two separate doublets broaden, coalesce, and finally sharpen again to give a still broad doublet (the broadening may be due partly to the fact that the boiling point of the solvent had been reached). The process is reversible and must involve intermolecular exchange of PF_3 between the two complexes. Approximate line-shape analyses of the spectra in the range 50–82° yielded rates of 20–250 sec^{-1} and a free energy of activation of 17.0 ± 0.5 kcal/mol. The intermolecular exchange may involve $Rh_2(PF_3)_5[As(CH_3)(C_6H_5)_2](C_6H_5C_2CH_3)$ as an intermediate, but the equilibrium, if it exists, is strongly in favor of the 1:1 mixture of hexakis and tetrakis complexes at ambient temperature.

***o*-Phenylenebis(dimethylarsine) (diars) Derivatives.** The bis(di(tertiary arsine)) derivatives $Rh_2(PF_3)_2(diars)_2$(ac) (ac = $C_6H_5C_2C_6H_5$ or $C_6H_5C_2CH_3$) show one widely spaced doublet due to $^1J_{PF}$ in their ^{19}F NMR spectra further doubled by coupling to ^{103}Rh (Table X); the spectra do not change on cooling to −77° ($C_6H_5C_2C_6H_5$ derivative) or −91° ($C_6H_5C_2CH_3$ derivative). The methyl resonances of the di(tertiary arsine) appear as two sharp singlets of equal intensity in the ^1H NMR spectrum of the diphenylacetylene derivative and as four equal singlets in the spectrum of the 1-phenylpropyne derivative (Table XII). If the molecules adopt an eclipsed conformation [as assumed also for $Rh_2(PF_3)_4[P(C_6H_5)_3]_2(C_6H_5C_2C_6H_5)$], there are three possible geometrical isomers, II a–c, for the phenylpropyne complex (R = C_6H_5; R' = CH_3); IIb and IIc become enantiomeric in the case of the diphenylacetylene complex (R = R' = C_6H_5). Clearly the methyl groups on each arsenic atom are inequivalent in IIa–c. When R = R', we therefore expect two methyl singlets in the case of IIa and four singlets for IIb or IIc, and when R ≠ R', we expect four methyl singlets for IIa–c. The possibilities of isomeric mixtures or of different orientations on the two rhodium atoms seem to be eliminated by the observation of only one P–F doublet. Although the NMR data fit structure IIa for the di(tertiary arsine) derivatives, one might have expected an $As(CH_3)_2$ group to have occupied the position held by triphenylphosphine in the $Rh_2(PF_3)_4[P(C_6H_5)_3]_2(C_6H_5C_2C_6H_5)$ structure. An alternative possibility which meets this objection is a mixture of IIb and IIc in rapid equilibrium. The exchange process could be a one-ended dissociation of the di(tertiary arsine) or partial rotation about the metal–metal bond. Since individual ro-

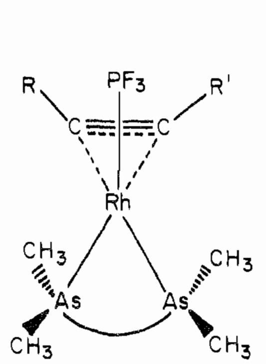

IIa

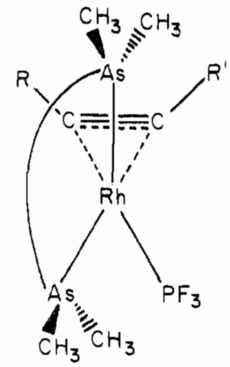

IIb

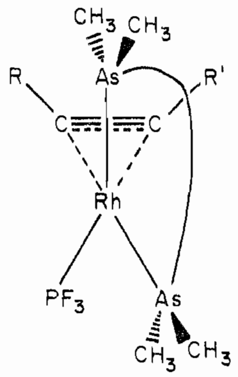

IIc

tamers are not observed for either of the complexes at low temperature, the free energy of activation for the process must be less than ca. 7 kcal/mol, which seems remarkably low in comparison with the values observed for the complexes containing monodentate ligands. The NMR results do not exclude structures containing two bridging di(tertiary arsine) ligands, but since the only example of a complex containing bridging diars is $[RC_5H_4Mn(CO)_2]_2$(diars) (R = H or CH_3),[34,35] these structures seem unlikely. At present, therefore, the structures of the $Rh_2(PF_3)_2(diars)_2$(ac) complexes are not known with certainty.

Acknowledgment. We thank the staff of The Australian National University Computer Centre for generous allocations of time on the Univac-1108 computer.

Registry No. $Rh_2(PF_3)_4[P(C_6H_5)_3]_2(C_6H_5C_2C_6H_5)$, 47913-68-8; $Rh_2(PF_3)_4[P(C_6H_5)_3]_2(C_6H_5C_2C_6H_5)\cdot(C_2H_5)_2O$, 38893-55-9; $Rh_2(PF_3)_4[As(C_6H_5)_3]_2(C_6H_5C_2C_6H_5)$, 56792-73-5; $Rh_2(PF_3)_4[P(CH_3)(C_6H_5)_2]_2(C_6H_5C_2C_6H_5)$, 56792-74-6; $Rh_2(PF_3)_4[P(C_6H_5)_3]_2(C_6H_5C_2CH_3)$, 56792-75-7; $Rh_2(PF_3)_4[As(C_6H_5)_3]_2(C_6H_5C_2CH_3)$, 56792-76-8; $Rh_2(PF_3)_4[P(CH_3)(C_6H_5)_2]_2(C_6H_5C_2CH_3)$, 56792-77-9; $Rh_2(PF_3)_4[As(CH_3)(C_6H_5)_2]_2(C_6H_5C_2CH_3)$, 56792-78-0; $Rh_2(PF_3)_4[As(C_6H_5)_3]_2$-*p*-$O_2NC_6H_4C_2CO_2C_2H_5$), 56792-79-1; $Rh_2(PF_3)_2(diars)_2(C_6H_5C_2C_6H_5)$, 56792-80-4; $Rh_2(PF_3)_2(diars)_2(C_6H_5C_2CH_3)$, 56792-81-5; $Rh_2(PF_3)_4[P(C_6H_5)_3]_2(CH_3C_2CH_3)$, 56792-82-6; $Rh_2(PF_3)_6(C_6H_5C_2C_6H_5)$, 38893-58-2; $Rh_2(PF_3)_6(CH_3C_2C_6H_5)$, 39015-25-3; triphenylphosphine, 603-35-0.

Supplementary Material Available: A listing of structure factor amplitudes (26 pages). Ordering information is given on any current masthead page.

References and Notes

(1) M. A. Bennett, R. N. Johnson, and T. W. Turney, *Inorg. Chem.*, **15**, 90 (1976).

(2) M. A. Bennett, R. N. Johnson, G. B. Robertson, T. W. Turney, and P. O. Whimp, *J. Am. Chem. Soc.*, **94**, 6540 (1972).

(3) The Busing and Levy programs [*Acta Crystallogr.*, **22**, 457 (1967)] were used for all phases of diffractometer control and data collection.

(4) Formulas used in the data reduction programs: *Lp* (Lorentz–polarization factor) = $(\cos^2 2\theta + \cos^2 2\theta_m)/[\sin 2\theta(1 + \cos^2 2\theta_m)]$, where θ and θ_m (=13.25°) are the reflection and monochromator Bragg angles, respectively; I (net peak intensity) = $[CT - (t_p/t_b)(B_1 + B_2)]$, where CT

is the total peak count in t_p sec, and B_1 and B_2 are the individual background counts in $(t_b/2)$ sec; $\sigma(I)$ (reflection significance) = $[CT + (t_p/t_b)^2(B_1 + B_2)]^{1/2}$; $\sigma(F_o)$ (the reflection esd) = $\{[\sigma(I)/Lp]^2 + (\rho|F_o|^2)^2\}^{1/2}/2|F_o|$; $\sigma_s(F_o)$ (the reflection esd from counting statistics alone) = $[\sigma(I)/2(Lp)(|F_o|)]$; R_s (the statistical R factor) = $\sum\sigma_s(F_o)/\sum|F_o|$; background rejection ratio = $[|B_1 - B_2|/(B_1 + B_2)^{1/2}]$.
(5) W. R. Busing and H. A. Levy, *J. Chem. Phys.*, **26**, 563 (1957); P. W. R. Corfield, R. J. Doedens, and J. A. Ibers, *Inorg. Chem.*, **6**, 197 (1967).
(6) "International Tables for X-Ray Crystallography", Vol. III, Kynoch Press, Birmingham, England, 1962, p 202.
(7) C. T. Prewitt, Ph.D. Thesis, Massachusetts Institute of Technology, 1962, p 163.
(8) D. T. Cromer, *Acta Crystallogr.*, **18**, 17 (1965).
(9) R. F. Stewart, E. R. Davidson, and W. T. Simpson, *J. Chem. Phys.*, **42**, 3175 (1965).
(10) G. B. Robertson and P. O. Whimp, *Inorg. Chem.*, **13**, 1047 (1974).
(11) C. K. Johnson, Report ORNL-3794, Oak Ridge National Laboratory, Oak Ridge, Tenn., 1965.
(12) U. Krüerke and W. Hübel, *Chem. Ber.*, **94**, 2829 (1961).
(13) Y. Iwashita, F. Tamura, and A. Nakamura, *Inorg. Chem.*, **8**, 1179 (1969).
(14) The method used to calculate weighted least-squares planes is described by D. M. Blow, *Acta Crystallogr.*, **13**, 168 (1960).
(15) W. G. Sly, *J. Am. Chem. Soc.*, **81**, 18 (1959).
(16) N. A. Bailey and R. Mason, *J. Chem. Soc. A*, 1293 (1968).
(17) N. K. Hota, H. A. Patel, A. J. Carty, M. Mathew, and G. J. Palenik, *J. Organomet. Chem.*, **32**, C55 (1971).
(18) D. Seyferth, R. J. Spohn, M. R. Churchill, K. Gold, and F. R. Scholer, *J. Organomet. Chem.*, **23**, 237 (1970).
(19) R. J. Dellaca, B. R. Penfold, B. H. Robinson, W. T. Robinson, and J. L. Spencer, *Inorg. Chem.*, **9**, 2197 (1970).
(20) R. J. Dellaca and B. R. Penfold, *Inorg. Chem.*, **10**, 1269 (1971).
(21) *Chem. Soc., Spec. Publ.*, **No. 18**, S17s (1965).
(22) G. B. Robertson and P. O. Whimp, *J. Am. Chem. Soc.*, **97**, 1051 (1975).
(23) D. A. Brown, *J. Chem. Phys.*, **33**, 1037 (1960).
(24) J. O. Glanville, J. M. Stewart, and S. O. Grim, *J. Organomet. Chem.*, **7**, P9 (1967).
(25) J. Dale in "Chemistry of Acetylenes", H. G. Viehe, Ed., Marcel Dekker, New York, N.Y., 1969, p 1.
(26) H. J. Goldschmidt and T. Land, *J. Iron Steel Inst., London*, **155**, 221 (1947).
(27) O. S. Mills and J. P. Nice, *J. Organomet. Chem.*, **10**, 337 (1967).
(28) C. H. Wei, G. R. Wilkes, and L. F. Dahl, *J. Am. Chem. Soc.*, **89**, 4792 (1967).
(29) Y. Morino, K. Kuchitsu, and T. Moritani, *Inorg. Chem.*, **8**, 867 (1969).
(30) R. L. Kuczowski and D. R. Lide, *J. Chem. Phys.*, **46**, 357 (1967).
(31) J. C. Marriott, J. A. Salthouse, M. J. Ware, and J. M. Freeman, *Chem. Commun.*, 595 (1970).
(32) K. Vrieze, H. C. Volger, and P. W. N. M. van Leeuwen, *Inorg. Chim. Acta, Rev.*, **3**, 109 (1969).
(33) M. A. Bennett, R. N. Johnson, and T. W. Turney, *Inorg. Chem.*, **15**, 111 (1976).
(34) R. S. Nyholm, S. S. Sandhu, and M. H. B. Stiddard, *J. Chem. Soc.*, 5916 (1963).
(35) M. J. Bennett and R. Mason, *Proc. Chem. Soc., London*, 395 (1964).

Contribution from the Research School of Chemistry, The Australian National University, Canberra, A.C.T. 2600, Australia

Preparation and Fluxional Behavior of New Rhodiacyclopentadiene Complexes Containing Trifluorophosphine

M. A. BENNETT,* R. N. JOHNSON, and T. W. TURNEY

Received June 3, 1975 AIC50380R

Dimethyl acetylenedicarboxylate, $CH_3O_2CC_2CO_2CH_3$, and methyl propiolate, $HC_2CO_2CH_3$ (ac), react with dirhodium octakis(trifluorophosphine), $Rh_2(PF_3)_8$, below room temperature to give red complexes of empirical formula $Rh_2(PF_3)_5(ac)_2$ (**1**, ac = $CH_3O_2CC_2CO_2CH_3$; **2**, ac = $HC_2CO_2CH_3$). Above room temperature explosive polymerization of the acetylenes ensues. The complexes are assigned a metallocyclopentadiene structure $(F_3P)_3Rh(\mu\text{-}C_4X_2Y_2)Rh(PF_3)_2$ (X = Y = CO_2CH_3; X = CO_2CH_3, Y = H) on the basis of ^1H and ^{19}F NMR spectra and a preliminary single-crystal X-ray study of the bis(triphenylphosphine) complex of **2**, the acetylene units in **2** being arranged in a "head-to-tail" manner. The $Rh(PF_3)_3$ unit in **1** and **2** shows fluxional behavior in the ^{19}F NMR spectra while the $Rh(PF_3)_2$ unit remains essentially unchanged, and an intramolecular tritopal rearrangement is suggested. Line shape analysis gives the free energy of activation ($\Delta G^\ddagger$) of the process in **1** and **2** as ca. 10.5 kcal/mol.

Introduction

In previous papers[1-3] we showed that a wide range of acetylenes (ac) react with dirhodium octakis(trifluorophosphine), $Rh_2(PF_3)_8$, to give binuclear complexes $Rh_2(PF_3)_6(ac)$. Single-crystal X-ray analysis of the bis(triphenylphosphine) derivative $Rh_2(PF_3)_4[P(C_6H_5)_3]_2(C_6H_5C_2C_6H_5)$[1,3] showed that the complexes are structurally analogous to the well-known cobalt carbonyl complexes, $Co_2(CO)_6(ac)$, obtained from $Co_2(CO)_8$ and acetylenes. The $Co_2(CO)_6(ac)$ complexes can react with an excess of acetylene to give complexes of empirical formula $Co_2(CO)_6(ac)_4$ or $Co_2(CO)_4(ac)_3$ in addition to cyclopentadienones, aromatic trimers, and polymers,[4] whereas, with only a few exceptions, the $Rh_2(PF_3)_6(ac)$ complexes are the only organometallic products which can be isolated from the reaction of $Rh_2(PF_3)_8$ with acetylenes. Two of these exceptions are dimethyl acetylenedicarboxylate, $CH_3O_2CC_2CO_2CH_3$, and methyl propiolate, $HC_2CO_2CH_3$, which form the subject of this paper.

Experimental Section

Experimental and spectroscopic procedures are as previously described.[2,3]

Preparations. *Warning*! The following reactions become violently explosive if carried out at or above room temperature. It is important to keep to the specified temperatures.

(Tris(trifluorophosphine)rhodia)(1–4-η-2,3,4,5-tetrakis(carboxymethyl)cyclopentadiene)bis(trifluorophosphine)rhodium(*Rh–Rh*), $Rh_2(PF_3)_5(CH_3O_2CC_2CO_2CH_3)_2$, 1. Dimethyl acetylenedicarboxylate (0.6 g, excess) was condensed onto solid $Rh_2(PF_3)_8$ (0.26 g) at liquid nitrogen temperature under a high vacuum. The mixture was allowed to warm to +20°C; gas (PF_3, ir identification) was evolved. The exothermic reaction was kept at or below 20° until no more gas came off. Unreacted acetylene was removed at 20° (0.005 mm) over a 12-hr period to leave a red solid which was extracted with four 5-ml portions of isopentane. The solution was filtered and cooled to −5° to give large red crystals of the complex, mp 162° (0.15 g, 58%).

Anal. Calcd for $C_{12}H_{12}F_{15}O_8P_5Rh_2$: C, 15.5; H, 1.3; P, 16.7; F, 30.6; mol wt 929. Found: C, 15.2; H, 1.4; P, 16.3; F, 29.8; mol wt (by mass spectrometry) 929. ^1H NMR (C_6D_6): δ 3.35 (s, CH_3); cf. $CH_3O_2CC_2CO_2CH_3$ δ 3.80. ^{19}F NMR data are in Table I.

(Tris(trifluorophosphine)rhodia)(1–4-η-2,4-bis(carboxymethyl)cyclopentadiene)bis(trifluorophosphine)rhodium(*Rh–Rh*), $Rh_2(PF_3)_5(HC_2CO_2CH_3)_2$, 2. The reaction was carried out as described above, unreacted acetylene being removed from the complex by trap-to-trap sublimation. The red solid when recrystallized from isopentane at −78° gave a 40% yield of the complex, which was further purified by vacuum sublimation.

Anal. Calcd for $C_8H_8F_{15}O_4P_5Rh_2$: C, 11.8; H, 1.0; P, 19.0; mol wt 813. Found: C, 12.3; H, 1.3; P, 18.7; mol wt (by mass spectrometry) 813. ^1H NMR (C_6D_6): δ 3.31 (s, 3, CH_3), 7.80 (m, 1, =CH), 8.24 (m, 1, =CH); cf. $HC_2CO_2CH_3$ δ 3.41 (s, 3, CH_3), 2.56 (s, 1, ≡CH). ^{19}F NMR data are in Table I.

(Bis(trifluorophosphine)triphenylphosphinerhodia)(1–4-η-2,4-bis(carboxymethyl)cyclopentadiene)(trifluorophosphine)(triphenylphosphine)rhodium(*Rh–Rh*), $Rh_2(PF_3)_3[P(C_6H_5)_3]_2(HC_2CO_2CH_3)_2$, 3. A solution of triphenylphosphine (0.38 g, excess) in *n*-pentane (15